CHALMERS

**Measurement System Design and
Experimental Study of Drive Train Test Rig**

Master's Thesis in the International Master's Programme in Applied Mechanics

JOSHUA CHRISTOPHER SQUIRES

MASTER'S THESIS IN INTERNATIONAL MASTER'S PROGRAMME IN APPLIED MECHANICS

JOSHUA CHRISTOPHER SQUIRES

Department of Applied Mechanics
Division of Dynamics
CHALMERS UNIVERSITY OF TECHNOLOGY
Göteborg, Sweden 2014

Measurement System Design and Experimental Study of Drive Train Test Rig

JOSHUA CHRISTOPHER SQUIRES

To my loving family, for your ever continued support in all my adventures

Measurement System Design and Experimental Study of Drive Train Test Rig

Master's Thesis in the International Master's Program in Applied Mechanics
JOSHUA CHRISTOPHER SQUIRES
Department of Applied Mechanics
Division of Dynamics
Chalmers University of Technology

Abstract

Of recent, there has been much research taken into the efficiency of extracting mechanical energy from renewable energy sources, in particular from the wind. Wind turbines have made much advancement in their operational uses, performance, longevity and efficiencies over the last couple of decades. Still however there is an underlying problem with the functional components of Drive Train System including the shafts, gearing and transmission.

Chalmers University of Technology has developed a modular test rig of a scaled down model simulating a direct drive wind turbine in partnership with leading industries. From this calibration of academia, industry and experienced professionals the test rig has been developed to its initial setup, a high speed subsystem. The rig was developed through study of existing test facilities included the National Renewable Energy Laboratory (NREL).

The test rig has been used by students from Masters level through to PHD level to analyse the performances and responses of a wind turbine under certain conditions and further research will continue to be undertaken for the foreseeable future.

Particular consideration has been taken into researching the dynamics of the system with particular attention made into the impacts of misalignment and the condition monitoring of the Drive Train System. Test rig properties were developed in AutoCAD® and Adams® and the computational understanding using Matlab® and SKF @ptitude Observer®. Paired with the use of accelerometers, displacement sensors and non-contact torque sensors allows for a wide range of studies to be undertaken.

KEY WORDS: Misalignment, Dynamics, Instrumentation, Vibrations.

Preface

The aim of this report is to deal with the advancements in wind turbine development at Chalmers University. It forms part of the ongoing research into wind turbine functionality that is supported by the Swedish Wind Power Technological Centre (SWPTC). This thesis focal point is on the implementation of instrumentation onto the operational test rig. In this setup the rig resembles a high speed shaft subsystem unit, simulating the stage of power generation present in a wind turbine. The design of this development has been conducted using both academic research and industry leading professionals, highlighting the key direction for its progression.

Göteborg June 2014

Joshua Christopher Squires

Contents

Table of Figures

1 Introduction

1.1 Background

It is imperative that further advancements be made in the field of renewable energy, in particular when it is extracted from the wind. A wind turbine operates to convert the potential energy of the wind into mechanical energy that can be used as power. High levels of research are currently taking place globally, both through academia and industry, all with a view of improving the lifespan and efficiencies of this conversion process.

Chalmers University of Technology has conducted research over the past decade into analysing the wind turbine in many differing ways. Particular attention has been directed to the impact of vibrations on the dynamics of the turbines operation. This has led to the development of a mounted modular test rig located in the Vibrations and Smart Structures Laboratory of the Division of Dynamics at Chalmers.

The wind energy market is emerging at a rapid rate both nationally and globally. Wind power accounted for 32% of the total new renewable power generation installed within Europe during the year of 2013 [2]. The European Union has already set in motion strategic plans to raise the share of renewable energy sources in the final energy consumption of the Union from 8.5% in 2005 to 20% in 2020 [3]. The annual investments in offshore wind farms averaged 5.5 billion Euros in the year of 2013, an increase of nearly 750% compared with a decade ago[2]. In the month of March 2014 it was reported that two projects involving the construction total of 326 wind turbines has been given approval off the coast of Scotland, it will stand as the third largest wind farm in the world. Expected to provide 2.5GW of electricity which it will deliver to more than a million homes while creating employment for 4,600 staff and generating around £2.5 Billion for the Scottish economy [4]. The European Wind Energy Associations announced in a recent report that Europe was the global leader in offshore wind energy in 2011 with 90% of the world's installed capacity. They are predicting that one quarter of all Europe's energy could be produced offshore [23].

It is clear that at this rate of development, technological advancements also have to be made. An advancement that has made considerable progression was developed in

response to the vast investments being made, a condition monitoring system that can assess the performance and reliability of the wind turbines operation through analysing the dynamics of the system over varying time periods. To operationally function, sensors are implemented onto and into varying components around the wind turbine which synchronously relay their data to the monitoring system. This system then analyses this data and creates performance reports for the technicians. The motivation for "condition monitoring systems" stemmed from several factors. Gearboxes in wind turbines have not been achieving their expected design life; however, they commonly meet and exceed the design criteria specified in current standards in the gear, bearing, and wind turbine industry as well as third-party certification criteria. Complete gearbox failures within a wind turbine are not too common, but are very costly to repair and rectify. This means that if there was a system that can detect faults at an earlier stage, complete failures can be avoided and some repairs can be planned ahead of time with minimal downtime, saving money.

The National Renewable Energy Lab (NREL) located in Colorado is leading the way in renewable energy initiatives. Funded by the United States Department of Energy the NREL received $328 million in 2009 [21], of which $55 million was directed towards the National Wind Technology Centre (NWTC) [22]. This centre is working towards identifying how gearbox misalignments can affect wind turbines operations [20]. Figure 1 shows a schematic for their test rig, although there work is on an international level it is important to highlight that having their research combined into a condition monitoring system would help alleviate the costly downtime reparation hours currently incurred across this energy sector.
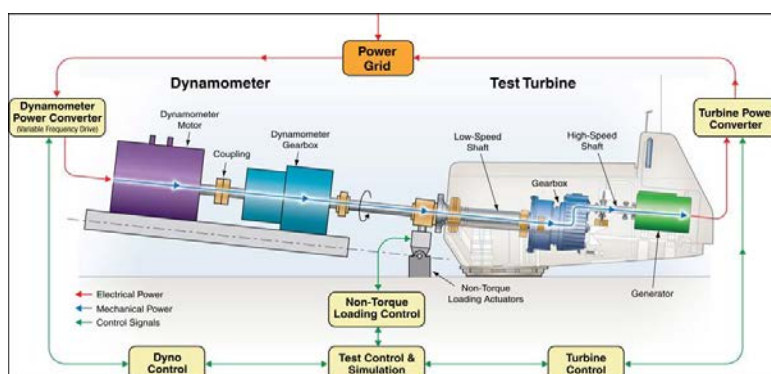
Figure 1: NREL [21]

1.2 Ongoing Model Development

In addition to the work carried out in this report there is an ongoing study taking place by a PHD student into the design and construction of a computational simulation model. This model aims to simulate the high speed shaft test rig dynamics with focus on misalignment analysis. EMC is the three step strategy that highlights how this simulation model is being developed and its connection with the test rig through the experimental data obtained. The results obtained from the combination of mathematical and experimental analysis will help new and improved designs for drive train components that enhance reliability and cost efficiency to be developed.

The process begins with the engineering model stage where the main design takes stage. After research into other test facilities designs had been undertaken, a suitable plan was developed and a scaled modular test rig was constructed. This engineering model now forms the basis for any developments and advancements that are made on the test rig and can be altered and edited using the programme Autocad®. The test rig during this report was designed up to a setup 1 level; this level represents a high speed shaft subsystem (HSSS). After analysis of this setup is complete construction will progress onto setup 2 where the system will represent a direct drive system (DDS). At this setup stage the motor and generator will have a direct connection. Post analysis design and construction advancements will be made to progress the test rig onto setup 3 whereby the system will represent an indirect drive system (IDS). There will be a gearing system present in this setup.

Progressing on from the engineering model is the mathematical model. This stage is crucial to the operation of the test rig and is where the equations of motions are considered. These equations are taken from the dynamic analysis of the test rig and are altered as the engineering model progresses. The reasons for these alterations stems from what is mathematically acceptable and what happens in reality. As an example, by considering a completely rigid shaft in the mathematical model this may not be the case in the engineering model in which critical scenarios, for example emergency shutdown, where extreme loadings take place. This mathematical model has been developed using the software Adams® which allows for fixed reference points and simulations of the engineering model to be analysed. Graphical data representation can then be extracted from this in order to determine certain characteristics of the test rig.

In addition to using the mathematical model it is also important to consider the computational model. This model forms the basis of the analysis and is used as a data interpretation process. Using a developed script in Matlab® it is possible to numerically analyse the response of the mathematical model. It is at this stage that will depict if the progress made has been successful. If for example the script creates graphical data that shows erratic behavioural response of the system then it identifies that alterations need to be made to the engineering model and the whole process repeated again.

1.3   Objective

The main motivation of this project is to understand the reason why faults and failures happen within the Drive Train System of a wind turbine and its functional components including shafts, coupling and gears. Utilising condition monitoring systems to Detect – Predict – Prevent is one key way to reduce the number of downtime hours that a wind turbine will face when faults and failures occur. The test rig is being developed in order to support the advancement of the mechanical models that can be used to improve existing CMS systems and develop newer and better ones.

This thesis is a continuation in the development of a scaled modular test rig. The direction is to develop and implement a measurement system, while ensuring that it delivers data which will be used for model validation and experimental investigation of the drive train system test rig. This includes the installation of probes, probe calibration and data acquisition routes setup. The use of tools for data analysis, experimental investigation of test rig frame response and the investigation into the assumptions made for previously developed mathematical models will be incorporated.

2 Hardware Available

The main hardware at this stage can be considered in groups from three perspective providers, ABB®, SKF® and National Instruments®, see Figure 2 for the labelled CAD model and physical model.
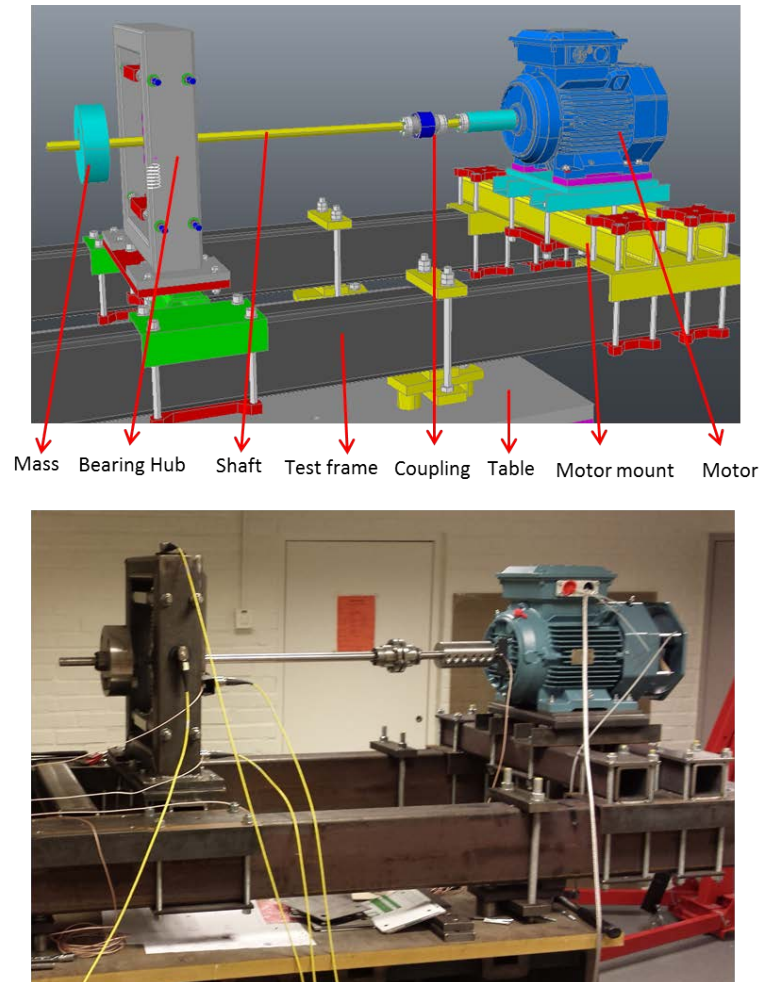
Figure 2: Details of test rig

ABB® has provided a considerable amount of equipment in donation to the projects development. A pair of 400V, 3 phase, and 6 pole induction motors act as the motor and generator in the wind turbine setup, see Figure 3. Capable of delivering shaft rotational speeds up to 1500rpm they are able to replicate the rotational speeds experienced with the main frame of a wind turbine [5].

Figure 3: ABB motor [5]

These motors are controlled by a pair of ACS355 motor controllers, see Figure 4. These controllers have been selected for their performance and longevity capabilities. They have been designed to deliver a range of variable parameters that will enable intricate analysis of the test rig to take place. Incorporated into this is the ability to conduct '*extreme limit testing*', the motor controller has the capabilities to deliver up to 75Hz to the motor allowing for a rotational shaft speed in excess of 1500rpm [1]. An operational scenario to this effect would simulate an '*extreme*' condition in reality.

The creation of a "common DC link" between the generator and motor was also another setup requirement. The concept of this "link" is that the power generated during the transition from motor to generator can be recirculated back into the motor. This prevents the need to "energy dump" which usually takes place in the form of heating resistors.

Figure 4: ABB ACS355 motor controller [1]

A fieldbus module acts as a plug-in module that allows for multiple system connections to be incorporated into the setup [6], see Figure 14. This unit will act to connect the motor controller with the National Instruments system route. An MTAC-01 extension module was also incorporated into the controller; this module serves the purpose of offering a pulse encoder interface allowing for motor rotational speed to be measured through data acquisition from the encoder, located on the back plate of the motors [7], see Figure 15.

Since this report is focussing on the development of the high speed shaft, one motor and controller is being used.

SKF® also exists as an industrial partner with Chalmers University of Technology and has equally donated a vast array of instrumentation towards the projects development. A set of six displacement probes and drivers, two high sensitivity accelerometers and two standard accelerometers, and all respective cabling were among the donation package. In addition to the sensors they generously gifted a Multilog system with corresponding software package (SKF @ptitude Observer®). Their full contribution forms one of the analysis routes being used within this project. A six day training and installation package was also offered, this enables Chalmers Test Rig project users to connect with SKF engineers to fully understand the installation, maintenance and operational uses of this system.

The IMx-P Multilog system [8] that SKF donated is an adaptable device that is used by many wind turbine operators around the globe. Also given the pseudonym "black box", it is a portable system that is used as an online data acquisition and analysis system. Containing 16 analog and 8 digital inputs it is a versatile device that assists in troubleshooting, condition monitoring and vibration analysis, see Figure 5.

SKF's donations of 6 * CMSS-65 5mm probes with the 6 * CMSS-665 drivers act as displacement sensors to the system and can be fitted in any position and direction to monitor the movements of any metal object [9], see Figure 6. They are contactless and have a read limit over a distance of 2mm from the measurement surface. They work using a magnetic field that is created around the surface of the probe, as the target object encroaches into this field, eddy currents are generated on its surface that decrease the field strength thus decreasing the drivers voltage output. It is this change in output voltage that can be graphically represented as the displacement of the examined member.

Figure 6: SKF displacement probe & driver [9]

In addition to the displacement sensing equipment it is also important to consider the accelerations that are occurring. To identify the occurrences of these accelerations SKF also contributed a pair of CMSS-799LF accelerometers and a pair of CMSS-2200 accelerometers. The CMSS-799LF set are highly sensitive, with a sensitivity level of 500mV/g, ideal for areas of the test rig that may experience small but notable vibrations, see Figure 8. Meanwhile the CMSS-2200's are a standard sensor operating with a sensitivity level of 100mV/g [10] see Figure 7.

Figure 7: Low sensitivity accelerometer [10]   **Figure 8: High sensitivity accelerometer [10]**

National Instruments® (NI) currently isn't an active external partner so the hardware listed was purchased from them using recommendations NI engineers had made. A Compact Data Acquisition (DAQ) system was used as the data acquisition base with a number of modules purchased to assist in the data extraction. One digital input/output module which should be used to relay the digital encoder signals, one analogue output module that acts as a digital to analogue converter used to carry the analogue motor controller signals, one analogue input module that acts as an analogue to digital converter used for the transmission of the analogue encoder signals and finally another analogue input module that would collate the four accelerometer signals. The compact DAQ system features an ethernet connection which connects directly into the computer for signal analysis [11], see Figure 9.

Figure 9: NI Compact DAQ [12]

Although this project features many items from a wide range of companies the main aim is still clear. To deliver a dual directional instrumented system, incorporating both the "Black Box" strategy that the SKF offer with the Multilog system, and the "NI System" strategy incorporating an array of modules and virtual interfaces in Labview, in order to analyse and assess the overall response of the HSS.

2.1 Sensor Choices

A total of ten sensors, including six displacement sensors, two high sensitivity accelerometers and two standard accelerometers, were received as part of the SKF donation package. As an initial plan a total of six of these sensors will be used, leaving the other 4 available for use when the DTS test rig is developed further.

The selection of sensors that were chosen was based on several factors, industrial recommendations, forming the first factor. It was important to consider all parties in the decision making process and identifying that the supporting external partners all specialise in the products that they manufacture. Their ideas were therefore very important when considering the progression of the test rig through each setup advancement made.

The next factor for consideration was the usability of the product. Requiring hard wearing, easy maintenance and reliable equipment was paramount. All equipment selected had to serve a multiple compatibility role because it was imperative that all systems could operate simultaneously and synchronously during the data acquisition process. It was important therefore that the products chosen prevented any data acquisition conflicts.

The final factor considered was financial. Although two of the operating systems being used were external partners to the project (ABB and SKF), the third system produced by National Instruments was not. This meant that as important as key component selection was, appreciation had to be given to the budget available for this project.

3 Software Available

There are currently three software packages that analyse the system and its responses, SKF @ptitude, Labview and Matlab.

3.1 SKF @ptitude

SKF @ptitude Observer forms part of a family of condition monitoring systems that SKF offer under their Windcon branch of operations [13]. The purpose of this branch within SKF is to extend the life of wind turbines through a number of operational capabilities. These operations achieve extended turbine longevity through predicting failures before they occur and by planning more effective maintenance schedules, thus reducing overall maintenance costs. By implementing sensors inside and around the wind turbine, data acquisition can take place relating to its operations. This data is stored and logged in the monitoring system, the IMxP-Multilog, which when connected with the @ptitude Observer software is capable of tracking many operational scenarios including gear damage, blade vibrations, misalignment, lubrication errors and bearing conditions. This @ptitude Observer software is at the forefront of analysis and has the capability to allow its users access to a fleet of wind turbines for periodic analysis in any remote location.

Its features include a vast array of analysis techniques, including FFT (fast Fourier transform) which uses a vibration signal as a function of frequency to identify faults. Time waveform analysis allows for the detection of waveform signature patterns in order to avoid error. Another analysis technique that is available is DPE (digital peak enveloping); this method can be used to detect very small but notable impulses that are occurring within a noisy environment. These analysis techniques along with all the others available within the @ptitude Observer software package work in unity to deliver the highest level of data interpretation and accuracy possible.

In conjunction with the many forms of analysis techniques available there is also a wide range of user interface displays contained within the Observer software. These act to graphically display the data either as a live feed or as a post processing technique. The author has listed several of these capabilities below;

Spectra: allows for fault comparison at specific event settings, for example it is possible to compare the faults occurring on the generator vertical bearing with any of the other bearings.

History/3D Plots: these methods display the variation in machine condition over time by allowing the comparison between visualization charts to take place helping to identify any impending faults.

Orbit/Profiling: these features will play an important role in future work carried out on this test rig. The concept is that two or three axis sensors can be mounted around a shaft in order to graphically determine unbalance and alignment problems.

All of these interfaces allow the users to clearly identify faults that occur around the turbine in a variety of scenarios and independently of one another.

3.2 Labview

Laboratory Instrument Engineering Workbench (Labview) [14] is a variable platform analysis software designed and developed by National Instruments (NI). It is identified as being a visual programming language that's functionality allows its operators to perform a variety of control and acquisition operations.

By utilising the data obtained from the bank of sensors located on the test rig, Labview has the capability to deliver graphical and numerical representations of this to give a visual understanding of the processes taking place.

The face of Labview is broken down into two interface sections, the first is the block diagram and the second is the front panel. The block diagram contains the graphical code used to operate the system, it is within this that modules, functions, terminals and wiring can take place. The concept is to create an operable system using a variety of tools that executes sequential operations creating a dataflow from start to finish. A complete selection of tools are available within the tool palette, it is from here that the code can be created that incorporates all the necessary terminals, controls, indicators, acquisition modules, timers and wires to create the VI. The front panel acts as a visual

for the block diagram created, it is here that the input and output displays can be coordinated.

3.3 Matlab

Matlab (Matrix Laboratory) is a software package for numerical analysis with programming capabilities, used globally for a range of purposes, which was developed by MathWorks [15]. The use of Matlab within this project will form the post testing analysis of the data as it is predicted that the data accumulated could far exceed the computational abilities of other software's such as Microsoft Excel.

4 Development Routes

As previously mentioned the instrumentation development of the project will take the form of two separate directions. One path follows the SKF system and the other, using the National Instruments system. Both paths were developed separately in order to allow for comparison of data analysis when experimental results are obtained.

4.1 SKF

The development of the SKF system began with the installation of the SKF @ptitude Observer Software onto the system. As previously mentioned, this software forms part of a network of SKF applications that unify as a monitoring suite. Its purpose is to provide a platform for engineers globally to conditionally monitor rotating machinery. This software is a comprehensive analysis package that allows its users to view a complete overview of the status of the wind turbine [13].

This software required a direct feed into a Microsoft SQL Express Server offering a 10GB storage database for the system.

The final stage of the SKF monitoring system is the Multilog IMx-P On-line System. Offering 16 analogue inputs and 8 digital inputs, this hardware will allow for simultaneous data acquisition to take place from the test rig and the sensors located on this. The hardware along with the @ptitude software package will provide several enhancing features to the operations of the HSS. The first is a fault detection function that activates through the use of alarms and warning icons to indicate to the operator that the system is experiencing dynamic instability. Secondly a fault prevention function that provides advice on correcting existing or impeding problematic conditions. Finally they will provide condition based maintenance analysis that will allow for improved reliability and performance. All of these systems operate simultaneously to give values for real time operational scenarios.

This route is used by many renewable power operators globally. Having it included in the operation of the test rig will help to identify key data parameters which can then be analysed on a secondary level by the National Instruments system.

See Figure 10 for a concise connection diagram of the SKF software listed above.
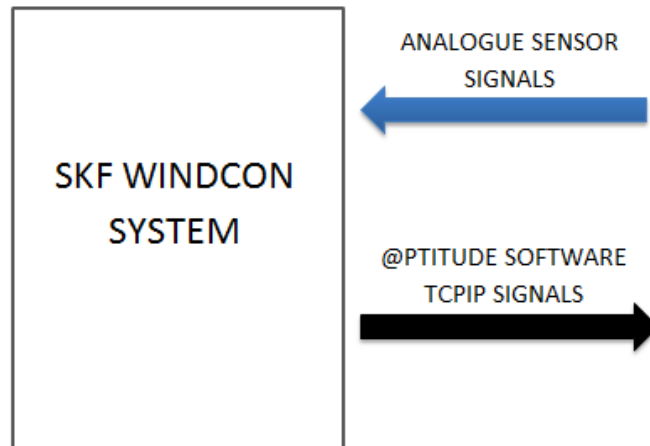
Figure 10: SKF software connections

4.2 National Instruments

The NI measurement system route begins at the sensors, similar to the SKF system, which are positioned around the test frame. These sensors then deliver the signals required for analysis from frame vibrations and displacements. This data is fed into a series of signal splitters that enable a connection to be made into the Multilog SKF system and also into the Compact DAQ Chassis. This forms the first stage of the NI route.

The second stage of this route takes place within the Compact DAQ Chassis which acts as an eight port terminal used in the data acquisitions process. This DAQ has installed a number of varying acquisition modules and terminals that are all used for a range of signals acquisitions.

From the Compact DAQ the signal data transport concludes in the software Labview. The connection between the hardware and software is made using a standard ethernet cable. It is in this software where all the data calibration and analysis takes place and it is predicted that similar responses to them found in the SKF @ptitude software can be achieved.

The software development of both SKF @ptitude and National Instruments Labview are discussed in a later chapter of this report.

4.3 Both Routes Combined

The reason for running an operational test rig with the two routes that have been discussed here is to create a fully examinable test rig, which uses both the leading technology that can be found in the field (Windcon) as well as the indirect analysis method (NI) that has been specifically tailored for this test rig. Another significant factor for incorporating the NI route is that the SKF system doesn't allow for direct motor control, whereas the NI route has both input and output capabilities, allowing for motor control and data extraction. The idea is to identify as accurately as possible the causes and effects of misalignment on the performance and reliability of a wind turbine in order to identify improvements that can be made to its existing design.

Figure 11 shows a full connection setup diagram that incorporates all three industrial contributors together.
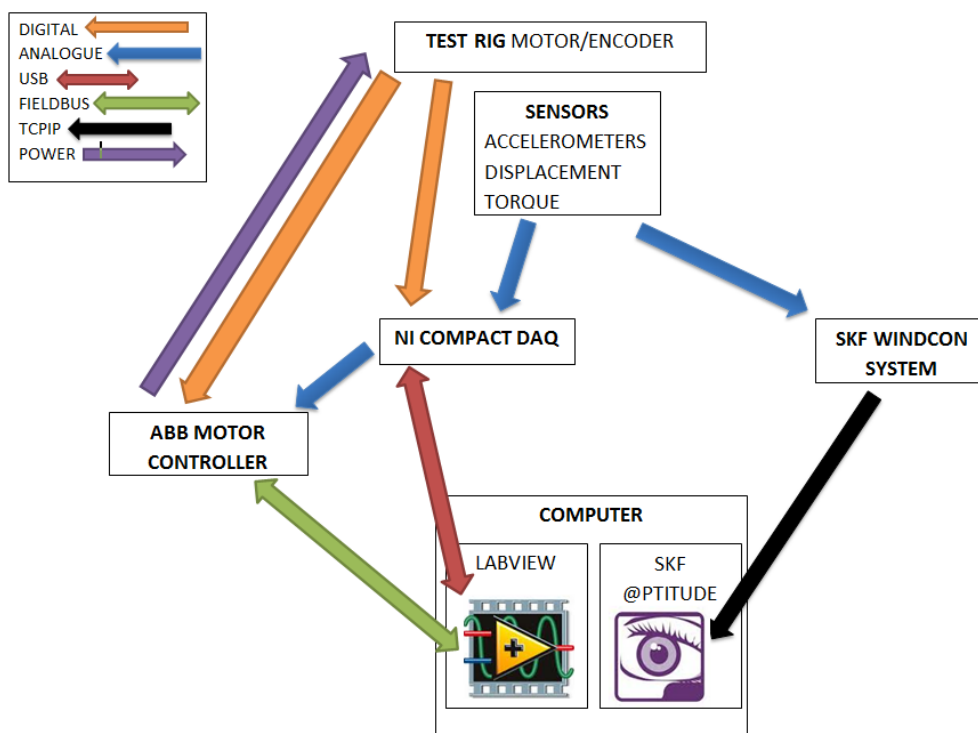

Figure 11: Full connection schematic

5 Software Development

This chapter will focus on the development of the two analysis software packages available, Labview and SKF @ptitude.

5.1 SKF

Installation of this software began under the supervision of an SKF software engineer who emphasised the importance of correct installation to avoid any malfunctions during the operational stages. The data acquired by the monitoring system can stretch the storage requirements into the gigabytes of data. In order to deal with this effectively it was recommended that a connection was established with an online server. Initially due to budgeting restrictions, this server took the form of a free Express SQL Server provided by Microsoft, this selection was made based on its ease of accessibility and the 10 GB of storage, per database, available [16]. The functionality of this allowed for immediate data recovery and a storage system that could be accessible anywhere and at any time. Once the test rig has reached its final setup then this server will be upgraded to a premium account with larger storage capabilities.

Post installation of @ptitude, access was made into the demonstration model account, this model acts as a template to allow its users to familiarise themselves with the software. Contained within this model were data sets that had been obtained by SKF from a BONUS 600kW turbine between the 4th May 2004 and 17th April 2005. This is a 44m tall turbine with an ABB Async driver unit that has been described as being one of the industry's most reliable turbines with over 2,700 operating around the globe [17]. This demonstration account also allowed the author to develop a better understanding and knowledge of the software's operations and how to use the integrated analysis tools contained within.

As part of the contributions to the development of this project, SKF have made considerable donations to its progress. As previously discussed a 6 day training package has been donated that will allow all operators of the test rig to spend 3 days in the laboratory with an engineering installation team from SKF, once completed a

further 3 days will be allocated to the software and data acquisition development. During this time a team of software engineers will begin the operation of the IMxP system. Upon training completion the SKF system will be fully functional and operational.

5.2 Labview

The development of Labview took place over a series of stages due to the level of complexity required for a full system acquisition. The initial development used was to develop the Author's understanding of this software. A basic VI was created containing a signal simulation and a graphical indicator, the idea was to understand the data flow using wiring and probes to graphically visualise the simulated signal. This VI was later enhanced to contain a series of numerical indicators, controllers, timers and loops. This development helped to intuitively identify more advanced software operations and highlight key improvement areas.

The idea was to take a systematic and methodical approach to the software development and so therefore further enhancement in this software occurred continuously throughout this project. In order to identify these key development areas, the aim is to systematically discuss these as they took place chronologically during this project.

One of the very first VI's created was constructed to allow for the testing of the accelerometers and displacement sensors. It comprised of a DAQ assistant pair and a set of waveform graphs that acted as a visual interpretation of the results obtained.

This VI then progressed onto the capability of writing data to a file while extracting the frequency response of the data obtained. This development occurred as a means of assessing the motor rotational speed.

It was decided that in order to efficiently select specific rotational speeds for analysis, an input controller should be incorporated into the VI. The use of a while loop in this VI also allowed for a continually varying input from the controller to be used.

The final development incorporated a "simulate arbitrary signal" into the system and a third DAQ assistant that was physically connected to the analogue output module used to control the motor. Having both systems contained within two separate while loops allowed for both stepped and ramped functions to be used as inputs, the final VI is shown in Figure 12.
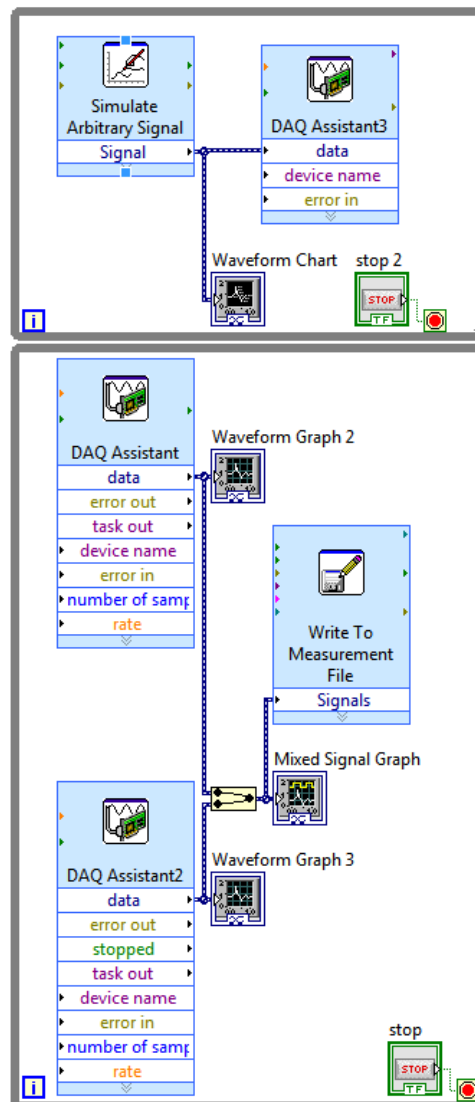
Figure 12: Final data acquisition Labview VI

A series of single VI's were developed throughout the course of this project that served the purpose of testing other system parameters. The first one developed had the purpose of allowing the knock tests to be carried out, containing a DAQ assistant, trigger and gate and a FFT module. This allowed for the creation of the knock test graphs seen later in the report. The other single VI used acted as an indicator for the shaft symmetry assessment that can be found later in this report.

6   Hardware Connections and Testing

The connections of the hardware into a the test setup took place over a series of developments, initially beginning with the testing and connection of the ABB controller and then progressing onto implementing the National Instruments setup.

6.1   Motor Controller Connection

The ABB ACS355 controller acted as a crucial piece of equipment within the system. It was therefore important to analyse the capabilities and performance of this controller before it was implemented into the full system setup. The motor controller connections are shown in Figure 15: MTAC-01 moduleFigure 13.
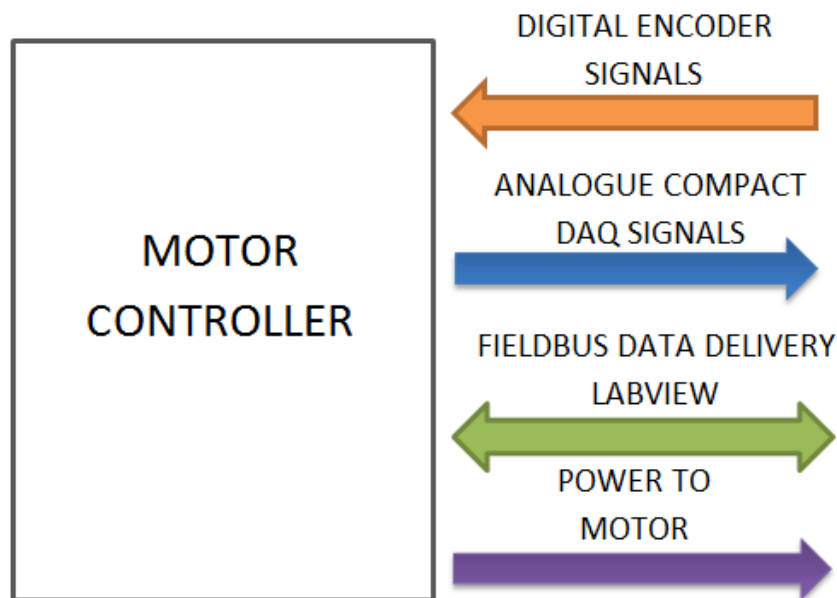
Figure 15: MTAC-01 moduleFigure 13: Motor controller connection schematic

To efficiently analyse the controller it was connected into the high speed shaft subsystem. The controller acted to process the signals and also as the power transmission from the mains power supply. It was important that it was therefore installed as instructed in the manual.

For the controller to perform to the requirements of this test rig additional modular units were required, see Figure 14 Figure 15.
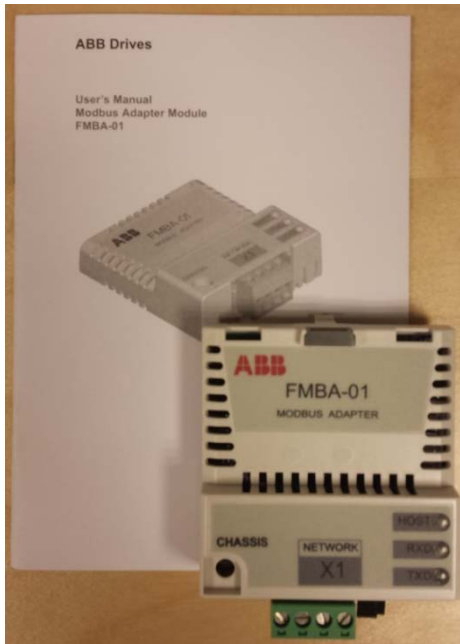
Figure 14: Field bus module

Figure 15: MTAC-01 module

The preliminary wiring of this system began with the installation of power input from the mains and the power output from the controller to the motor. This wiring took the form of a quad-core shielded cable which was used to reduce interference from other neighbouring electrical/mechanical machinery. Figure 16 is an image of the Delta setup that was required when connecting the power source to the motor.

Figure 16: Motor wiring - delta setup

After the connection of the power to the controller unit the next stage was the connection of the controller to the motor's encoder. The Leine-Linde encoder uses photoelectric scanning on a graduated code disk to deliver dual purpose information to the controller unit [18]. The information generated can relate to the measured

rotational speed or the relative coordinate position. The scanning detects lines on the code disk that measure a few micrometers wide and generates signals based on whether the light passes through the code disk or not. The generated signal is then directly fed into the controller unit which processes these signals and generates a visual value for shaft speed.

The connection of the encoder is shown in Figure 17. A note was made of the eight colour coding system used for future reference.
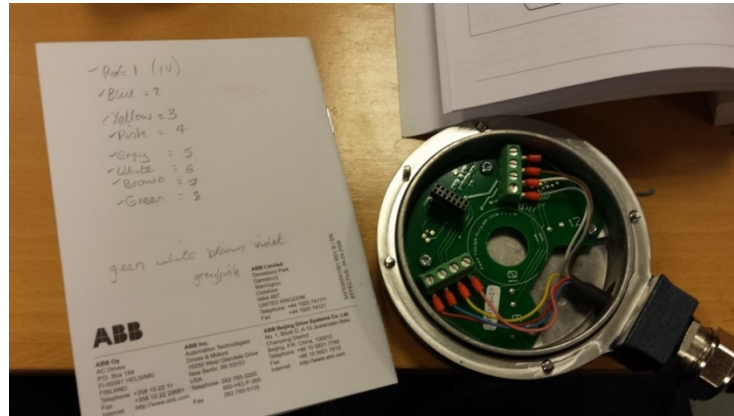

Figure 17: Encoder connection

The inner plate details are shown in Figure 18. Post wiring the encoder was then reconnected to the motor housing as shown in Figure 19.
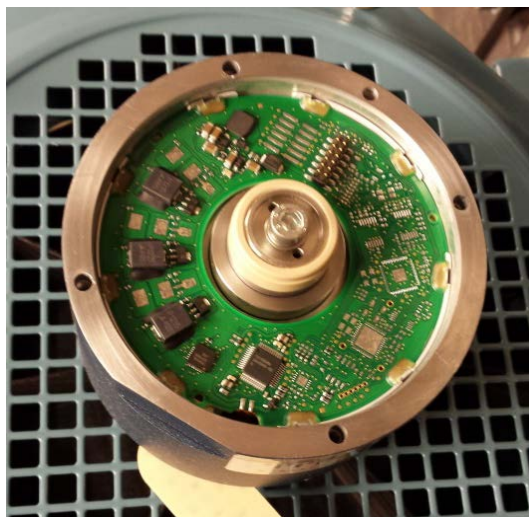

Figure 18: Encoder- open

Figure 19: Encoder- detailing

With all the preliminary wiring completed, it was important to focus on the controller wiring. Figure 20 below shows the wiring of the controller with the power output and the encoder connected.

Figure 20: Fully connected motor controller

The powering from the mains is shown in the far left connecter and situated next to this is the power delivery to the motor. As previously described the encoder is connected into the MTAC module using the same eight colour coded wires noted on the encoder. An additional connection required that power was also connected from the controller unit into the MTAC-01 using single core wiring.

The hardware development to this stage was considered an initial phase. This development allowed for significant testing of the controller including its interface, pre/programmable features and also its basic operations to be conducted. The motor could be turned on, speed up/down and stopped in this configuration.

Importance was stressed on the analysis into the performance of the controller unit and the only achievable way of reaching this was to adapt this current setup to allow a measurement system to be implemented.

The idea progressed into the connection of an oscilloscope and DC function generator onto this setup. Connecting the DC function generator allowed for a controlled signal delivery to take place to the motor via the controller. The DC generator was connected

into channel one of the oscilloscope and the encoder input "Sref" (in this instance Brown) was connected into channel two. It was imperative that the voltage delivery to the motor remained positive to prevent damage and this was controlled using the DC frequency generator. Figure 21 shows the setup that was achieved.
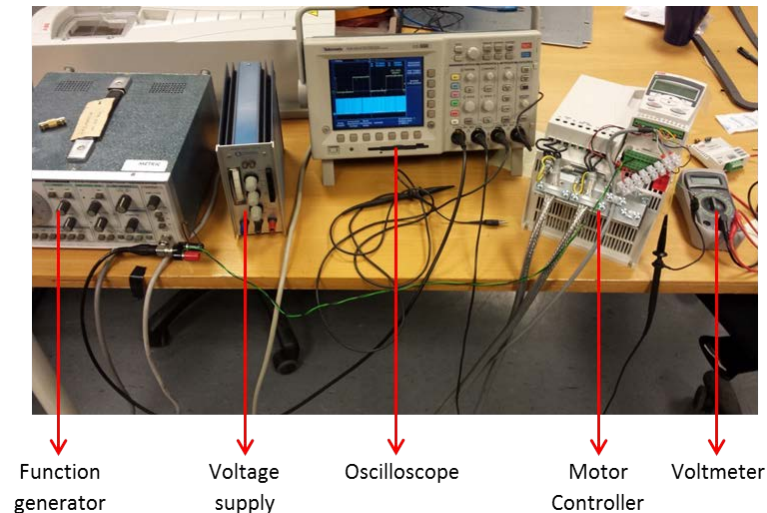
Figure 21: Wired setup 2

The hardware development to this stage was a secondary level stepping point. It was concluded that the frequency controller was very versatile in its usability and functionality containing a wide range of parameters. The problem that arose from this setup related to the performance analysis in the oscilloscope. The oscilloscope contained a very small recordable memory which meant that it was impossible to justify the performance level from the immeasurable number of encoder pulses achieved per revolution.

This led to the conclusion that in order to analyse the system fully, the next step was to develop and run this operational scenario from a Labview VI programme. This would allow for an infinite recording time and a greater accuracy when analysing the controllers' performance. Before this was carried out it was important to consider the other hardware that was going to be used in conjunction with the motor controller, such as the Compact DAQ.

6.2 DAQ Connections

As previously described a series of modules had been purchased from NI. These modules were housed within the Compact DAQ Chassis.

All four modules were connected into the Compact DAQ were then connected to the computer using an Ethernet cable. This ethernet connection created a live data feed directly into the computer where the signal analysis could take place in Labview. A new VI was created to help analyse the effectiveness and compatibility of each module which assisted in the understanding of the data feeds that were generated. Labview was used to act as an intermediate stage for data analysis with further analysis taking place using Matlab scripts, see Appendix file 3 for Matlab script developed. Figure 22 is a graphical representation of how the individual modules and terminals were connected into the Compact DAQ Chassis.

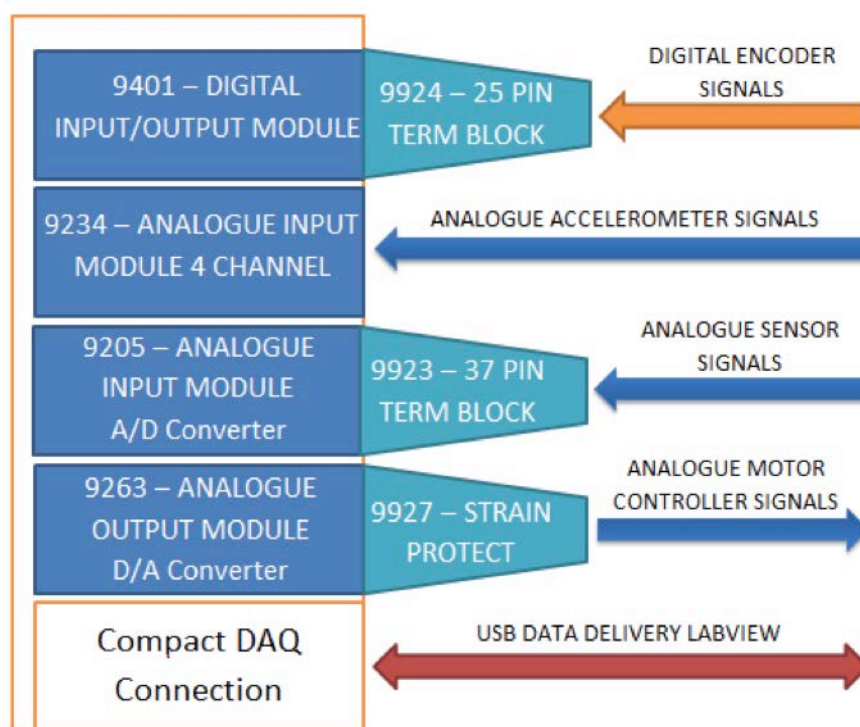**Figure 22: Compact DAC connecticvity schematic**

The first VI test began on the analogue input module (NI9205) see Figure 23. As the analogue input module this was considered for the first test because it required the addition of the 37 pin terminal block NI9923. This module is used as an analogue to digital (A/D) convertor which is used to deliver the analogue sensor signals into the analysis software.

The aim of this initial test was to deliver a signal from the DC generator into the NI 9923 terminal block, through the A/D convertor module, into the compact DAQ and then to Labview where the signal could be verified and visually displayed.
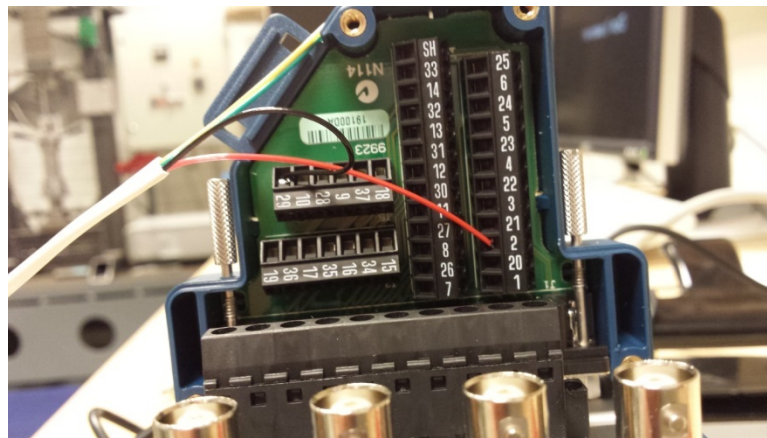

Figure 23: NI9923 module wiring

Terminal 29 (black wire) was connected to the ground port on the DC generator and terminal 2 (red wire) was connected to the +Ve port. The system was delivered with 100Hz from the generator, see Figure 23. The testing was now able to progress onto the Labview stage.

Initially using National Instruments Measure and Automation Explorer (NI-MAX) software the author was able to test the overall setup for signal delivery. This showed a successful signal delivery from all devices connected in the loop. Figure 24 below shows the module connection into the NI-MAX software and Figure 25 shows the first basic "on-off" test explored.
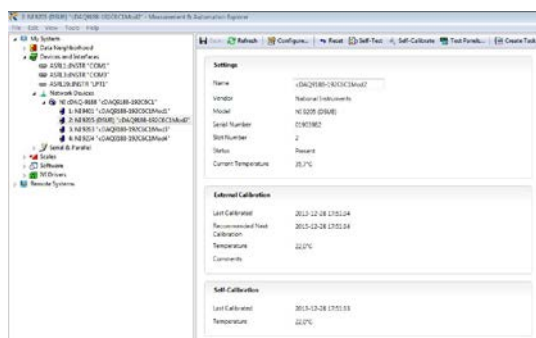
Figure 24:NI-MAX to NI9923 module connection
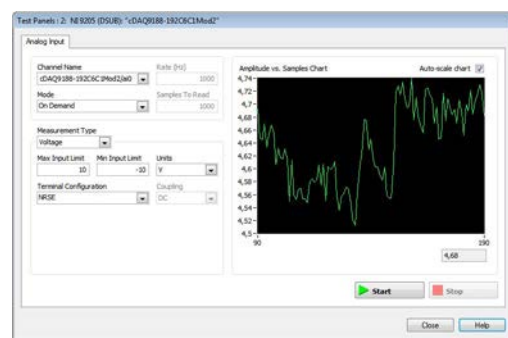

Figure 25: NI-MAX to NI9923 module testing

After clarifying that there was a clear signal a visual interface was created in Labview. Using a while loop, DAQ assistant and a waveform graph it was possible to visually interpret the signal that was being sent from the DC generator to the Compact DAQ and through the use of a while loop, this meant the data acquisition was continuous, so

the graph acted as a "live feed" when the frequency was altered. Figure 26 shows this result:
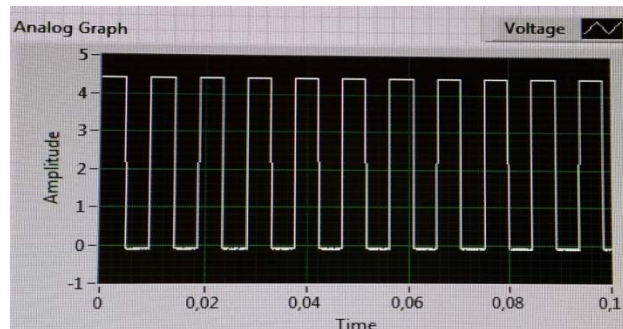
Figure 26: NI9923 module response

After this test proved to be a success analysis into the NI9401 module was made. Similar to before this module also had the addition of a 25 pin terminal block NI9924. The module will be used to deliver the digital encoder signals into the analysis software.

The purpose of this second test was to test the digital signal flow of the system. This terminal block and module would be used in connection with the encoder so its operation was vital to analyse the motors operation. The wiring for this module is shown in Figure 27.
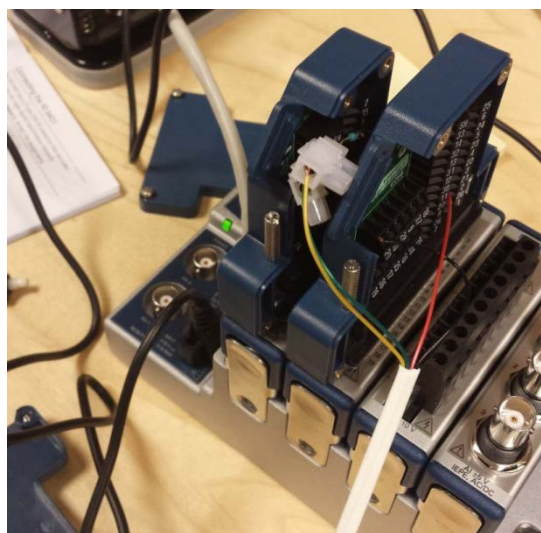
Figure 27: NI9401 module wiring

This module was also connected to the DC frequency generator which was used to deliver the same signal that the analog module was receiving. The terminal line DIO0 terminal 14 (green) was connected to the +Ve port of the generator and COM terminal 1 (yellow) was connected to the ground port of the generator. Before the two wires were connected into the terminal it was important to protect the system from over

powering and reverse polarity changes so two 1k resistors were wired into the terminals along with a diode.

Similar to the previous method this was connected to the NI-MAX software to verify the signals being generated, Figure 28 below shows the module connection into the NI-MAX software. The results this time was a green flashing LED, which varied in flash rate depending on the frequency delivered to the system, see Figure 29
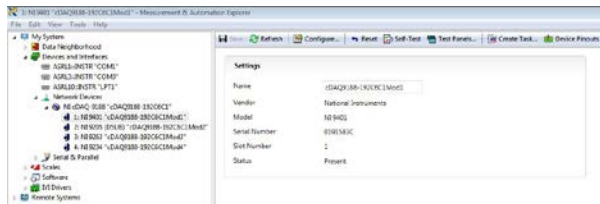
Figure 28: NI-MAX to NI9401 module connection   **Figure 29: NI-MAX to NI9401 module testing**
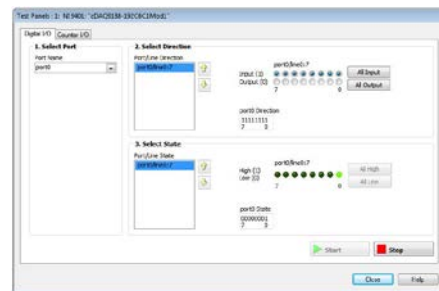
After clarifying that there was a clear signal, a visual interface was created in Labview. This was carried out the same was as before by inserting a DAQ Assistant into the while loop that had been previously created and used for the analogue module. Using a digital data waveform graph it was possible to visually see the pulsating response that was being delivered to the setup. This is shown in Figure 30.
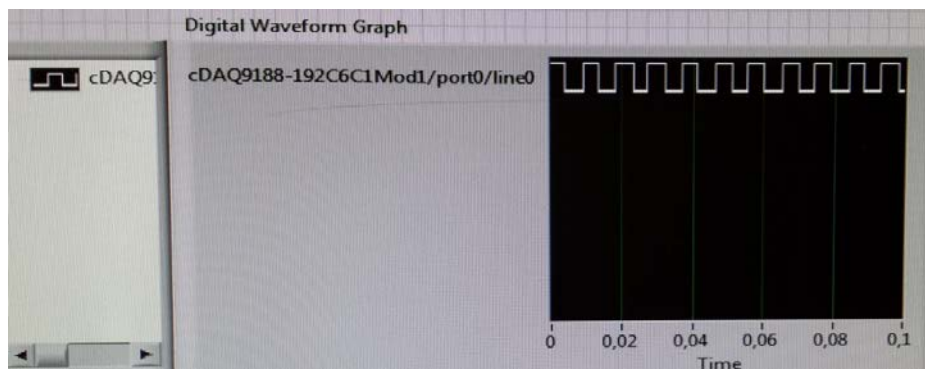
Figure 30: NI9401 module response

After this proved successful the terminal was rewired so that the connection was fed into the motor controller. This allowed for the signal delivery to take place from the motor controller, meaning that it was no longer necessary to use the artificial signals that had been generated by the DC function generator.

After this was completed it was decided to move onto analysing the analogue output module NI9263 with operational protector NI9927 casing. The purpose of this module

was to deliver the analogue motor controller signals from the analysis software to the motor controller which in turn was connected to the encoder. This could be described as allowing the user to control the motor operation from Labview.

Similar to the previous cases this was initially tested in the NI Max software to clarify that the signal was active through the Compact DAQ. See Figure 31 for the module connection into the NI-MAX software and Figure 32 show the first test conducted.
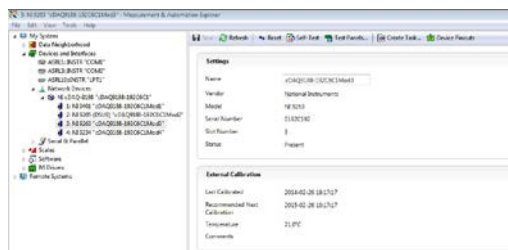
Figure 31: NI-MAX to NI9263 module connection   **Figure 32: NI-MAX to NI9263 module testing**
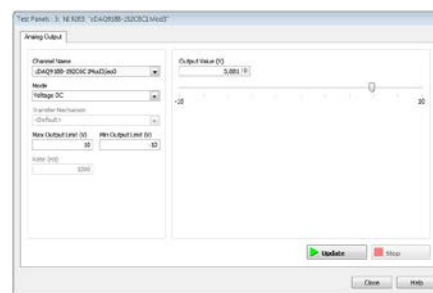
After this clarification another DAQ Assistant was created to act as a control for this module. This time it was required to generate a signal to deliver to the motor. The idea was that in delivering an analogue signal as an output from Labview it would be possible to visually see the response of the motor rotating.

In order to achieve this, a signal module and slider were incorporated into the Labview while loop which was then wired as the data feed into this new DAQ Assistant. The decision for this was to deliver a variety of signals from this module to the motor. Altering the wave type, frequency, amplitude and offset were just some of the variations that could be used as inputs to the motor. Before the signal was fed into the data feed a waveform chart was wired into the circuit, this allowed a visual representation to be given in addition to the visual and audio changes that the motor was making. Figure 35 shows this visual response and virtual wiring that was used in the block diagram.
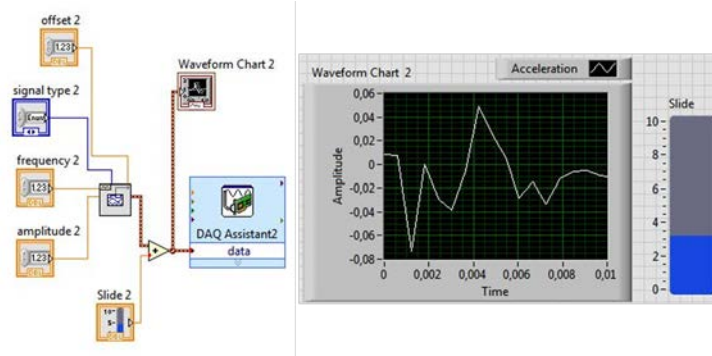
Figure 33: Labview motor output control VI

After this test had proved successful a decision was made to replace all of the inputs to the DAQ Assistant shown in Figure 33**Error! Reference source not found.** above into this module with a single "simulate signal" module. This would then allow for a variety of signals to be delivered to the motor including saw tooth, square and sine waves. Figure 34 is a photo showing the combined VI in Labview used to test the first 3 modules.
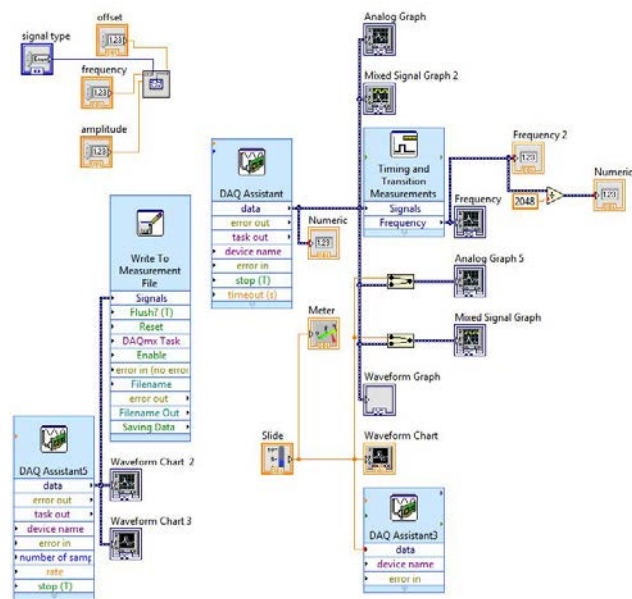
Figure 34: Three module analysis Labview VI

The final module that required analysis was the NI9234 analogue sensor input used to transfer the signals from the accelerometers into the Compact DAQ. The analysis of this module occurred during the testing of the accelerometer sensors phase. This can be found later in this report.

7   Sensor Testing

7.1   Pre-Testing

The pretesting phase was used to survey that everything was working as intended and to identify any potential errors that could have arisen from incorrect wiring or VI development. To isolate these problems the test rig was tested under several operational scenarios and the data outcome monitored. The key to this analysis was to assess whether there was any inconsistencies with the data that was extracted from the system through Labview. These operational scenarios included a stepped speed input as well as a ramped speed input.

As part of the pre-testing procedure an idea was developed to fit the accelerometers to magnetic foot plates. This would allow them to be repositioned anywhere around the rig during testing. By allowing for relocations around the test frame it allowed for extensive data acquisition to take place with minimal damage to the frame having to take place. Figure 35 shows these magnets and respective accelerometers.

Figure 35: Magnetic foot plates

7.1.1   Accelerometers

As previously discussed the final module, NI9234 analogue sensor input module still required its preliminary testing. The module would act to relay the data from the accelerometers into Labview for analysis. This pre-testing was undertaken when the sensors were tested, as they were the required input for this module.

The NI9234 analogue input module served the purpose of delivering the data that was acquired from the four accelerometers. The module worked on a simultaneous

acquisition level from the four sensors, meaning that all data was collated in the same instance.

For this pre-test of this module a CMSS 2200 Standard Accelerometer was attached to a magnetic foot and was connected into the module using one of the CMSS 932 cables. The author decided that because this was a testing stage that it was important to maximize the vibrations, so a lateral hand movement was made to ensure that large vibrations were achieved. A photo of this connection is shown in Figure 36.

Figure 36: Accelerometer connection

Unlike previous test procedures, this setup didn't require an NI Max pre-state test, instead a new DAQ Assistant was wired into the while loop as with similar cases. This was then linked to the physical channel "ai0" which was the connection port located on the module, the configuration method was for acceleration responses and a waveform graph was wired into the assistant. This configuration is shown in Figure 37.
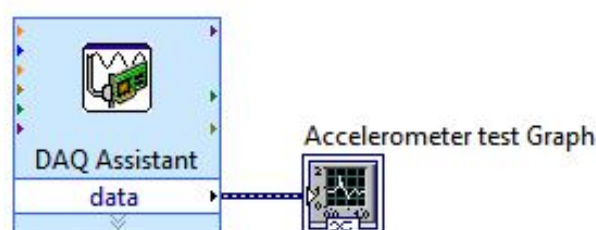
Figure 37: Accelerometer testing VI

The system was then initiated and the VI was run to acquire the data feed, the accelerometer was held and moved laterally at a rapid rate. The idea behind this was to maximise the vibrations within the accelerometer, this would then accentuate the graphical representation.

After this had been conducted, the magnet was positioned on the foot plate of the motor. This was now an area of significantly lower vibrations compared to the hand

movement, so it was crucial to test how responsive the accelerometers were. The graphical data that was fed back is shown in Figure 38.
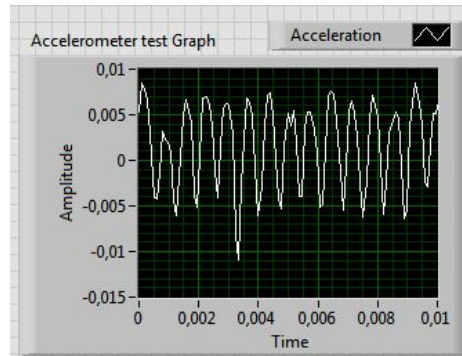
Figure 38: Accelerometer graphical response

With all modules having been tested on the National Instruments setup it was time to progress onto testing the SKF probes and displacement sensors.

7.1.2   Displacement Probes and Drivers

In order to assess the usability and effectiveness of the displacement sensors it was decided that they should be tested in a controlled scenario where all factors could be monitored. The process of this preparation is listed below.

Development began with the wiring of the probe to the driver and to the voltage generator. The driver required a voltage of 24V, since none of the other systems operated with this voltage, a generator was required. Figure 39 shows this unit.

Figure 39: Thandar voltage generator

The unit was set to deliver a voltage of 24V and a current of 0.12 amps; this was the required current to overcome the impedance of the system. The positive and negative terminals of this generator were then connected to the driver ports. The negative terminal wired to the -24V port and the positive terminal to the GND port. With the driver now receiving the required voltage it was time to consider the wiring into the Compact DAQ.

The operating voltage limit for the Compact DAQ was 10 Volts so it was important that the voltage was stepped down before being connected into the DAQ. Using a voltage divider rule from Ohms Law, see equation 1, was the way of achieving this.

$$(Eqn\ 1) \qquad\qquad V_{out} = V_{in} * \frac{R_2}{R_1 + R_2}$$

Knowing that a V_{out} value of greater then 10V couldn't be exceeded, a 15kΩ and 10kΩ were wired in series with the two output terminals. This would allow the 9.6V input to the Compact DAQ to be achieved. See Figure 40 for the wiring.

Figure 40: Displacement probe and driver wiring

7.1.2.1 Pre-Test Vertical

In order to better understand the probe response, a test was carried out that varied the probe displacement whilst recording the voltage obtained. This was undertaken to help identify the response of a probe to movement through its magnetic field in the vertical direction. The results of this could then be used to assess at which displacement the most accurate data acquisition would occur. Figure 41 shows this testing setup.
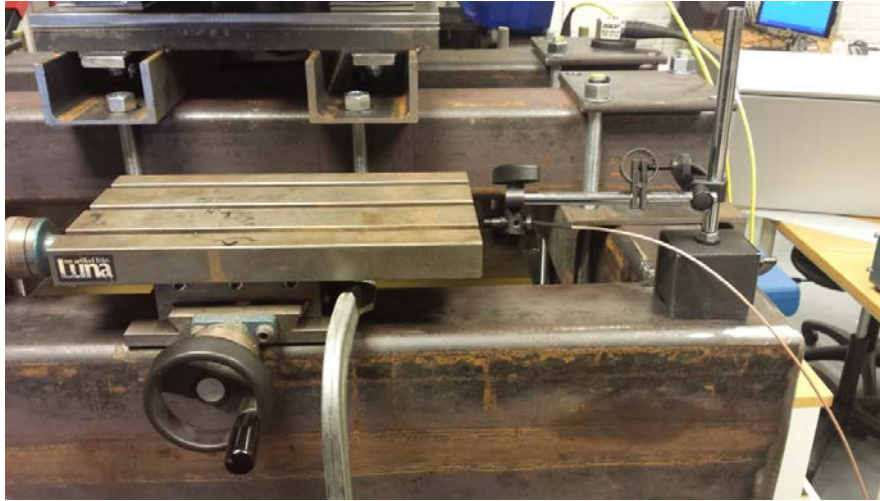
Figure 41: Vertical probe analysis
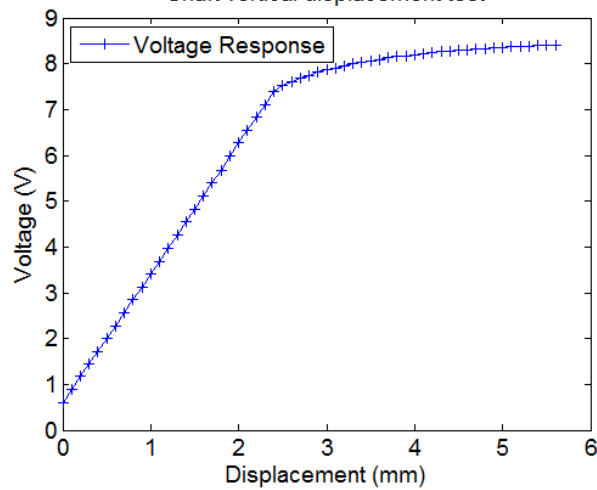
Figure 42: Vertical probe analysis response

From the graph shown in Figure 42 it can be concluded that the response of the probe follows a linear trend until 2.4mm offset when the shafts interaction with the magnetic field started to dissipate. The key identifier from this is that to maximise the accuracy of the data acquired the probe should be displaced approximately 1.2mm from the surface of the shaft. This would then allow for a shaft displacement of ±1.2mm in the vertical or horizontal direction before the magnet field was lost, or physical contact with the displacement probe head was made.

Using these recorded values it was possible to calculate that a voltage alteration of 1V within the test data corresponded with a displacement change of 0.361mm.

7.1.2.2 Pre-Test Lateral

Another consideration before experiment analysis could take place was for the effects of circumferential curvature on the response of the displacement probe. For this experiment a segment of the shaft was positioned on a coordinate axis test frame. Increments of 0.1mm movement laterally were made and the voltage was recorded, see Figure 43 for the testing setup.

Figure 43: Curvature probe analysis
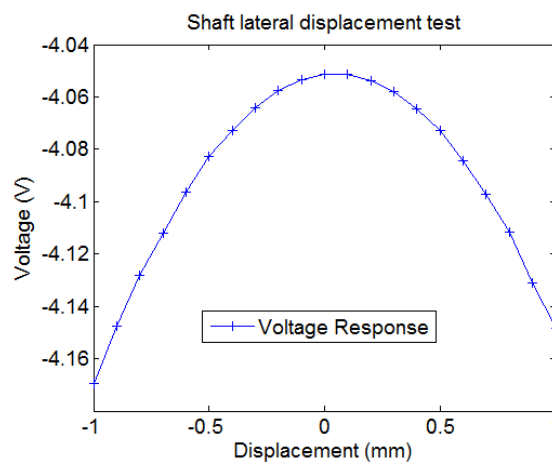
Figure 44: Curvature probe analysis response

From the graph shown in Figure 44 it can be concluded that the curvature of the shaft surface does have a slight impact on the voltage values obtained. With a shaft diameter of 30mm, lateral displacements of 0.5mm from the origin can be identified which would constitute to a voltage alteration of 0.03 volts. Consideration during future testing of the voltage changes and displacements were required to see if these correlated to any significant alteration in the shafts lateral positioning.

7.1.2.3 Key Lock Test

With the preliminary tests now completed it was time to install the probe onto the DTS setup to test its usability. Using the following setup of brackets and magnets it was possible to get the probe to be positioned within 1.2mm of the rotating shaft. Figure 45 shows this setup.
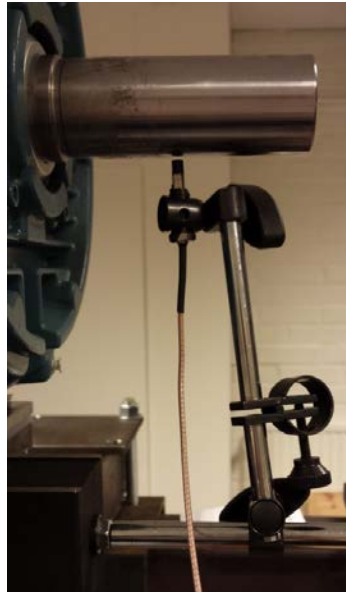
Figure 45: Key lock testing setup

With all of the equipment now into its correct wiring state, the software setup could then be altered to allow for correct data acquisition. The first step was to alter the existing analogue input module two DAQ Assistant to allow the flow of data through the system. The internal settings of this were altered so that the data acquisition could take place from "ai3" which was the channel line this sensor had been wired into. The rest of the Labview setup was left at its current state. The reason for this was that existing graphs could be used to perform the same visualisation response as was used on previous module tests. The Labview setup is shown in Figure 46.
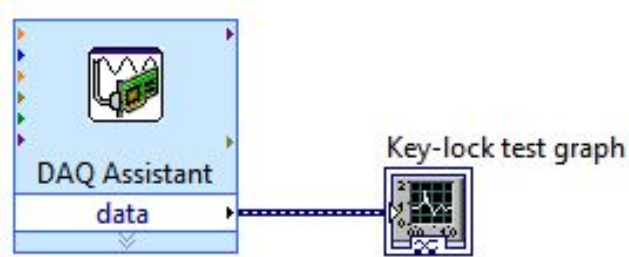
Figure 46: Key lock testing VI
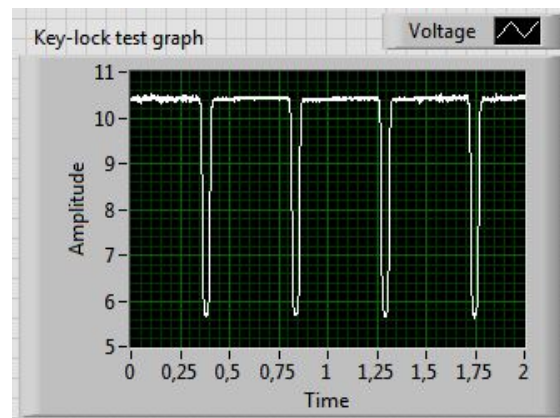
Figure 47: Key lock graphical response

The graphical data obtained is shown in Figure 47 shows a very small amplitude change initially followed by a vertical drop. The reason behind this was because the sensor was located directly under the key lock of the motor shaft. By positioning the sensor here it was possible to calculate the speed of the shaft by assessing the time alterations between these "pulses". With this test complete, and a satisfactory data extraction complete, it was possible to move onto examining where the sensors should be located.

8 Hardware Additions: Safety frame and Bracket Arm

The positioning of the sensor system was an important consideration because it would form the structure for the system dynamical analysis. Figure 48 was created as a conceptual positioning idea. Two of the displacement sensors positioning were analysed by a previous Erasmus exchange student and it was concluded that their vertical and lateral positioning at the bearing hub would deliver the greatest response accuracy. The previous exchange student had proposed that the sensors should be fixed onto the bearing unit.

After further investigation it was decided that the seating of these sensors in these positions would invalidate the data. The reasoning concluded was as higher eccentric masses are tested and the bearing house damping system experiences greater levels of displacements the probes will still be recording zero amplitude change. If both the shaft and displacement sensors are fixed in position to one another then the data obtained will always be constant in magnitude.

The alteration to the original design, attaching the probes to a pre-welded bracket arm, would act to remove any external vibrations that the displacement sensors could face if they were mounted onto the bearing housing unit. Appendix file 1 shows a full CAD drawing of the bearing hub and bracket arm.
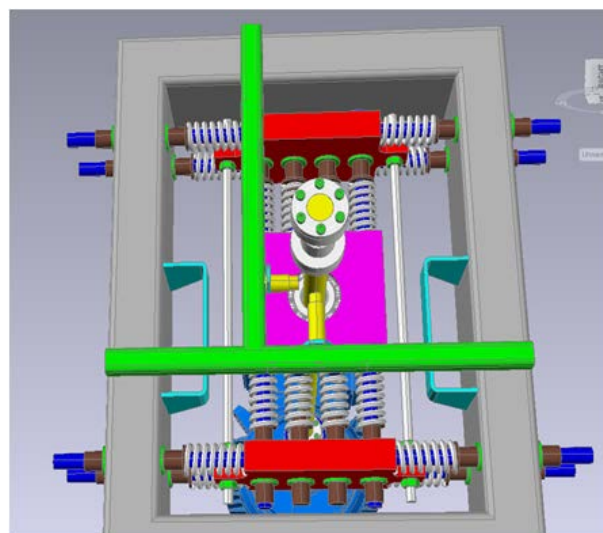

Figure 48: Virtual bracket arm design

In order to achieve successful displacement analysis of the shaft, the displacement probes will have to be positioned within the 2mm required range specified on their data sheets. In conjunction with the Vertical test that had been previously undertaken it was concluded that a 1.2mm positioning from the shaft would allow for the widest

displacement ranges to be recorded effectively. The actual frame that was constructed from the model is shown in Figure 49.

Figure 49: Actual bracket arm design

In addition to the design required for the displacement probes bracket arm, consideration also had to be made into the safety of the test rig operators. With a mass of 20kg rotating at 900rpm there were safety concerns created which led to the design of a structural safety frame. The conceptual idea created consisted of two separate frames that were positioned on rollers. This was to generate a safe working environment whilst allowing maintenance and alterations to be made to the test rig easily by sliding the casing on its rollers. The CAD concept shown in Figure 50 shows the design created; this can also be seen as a CAD drawing in Appendix file 2.
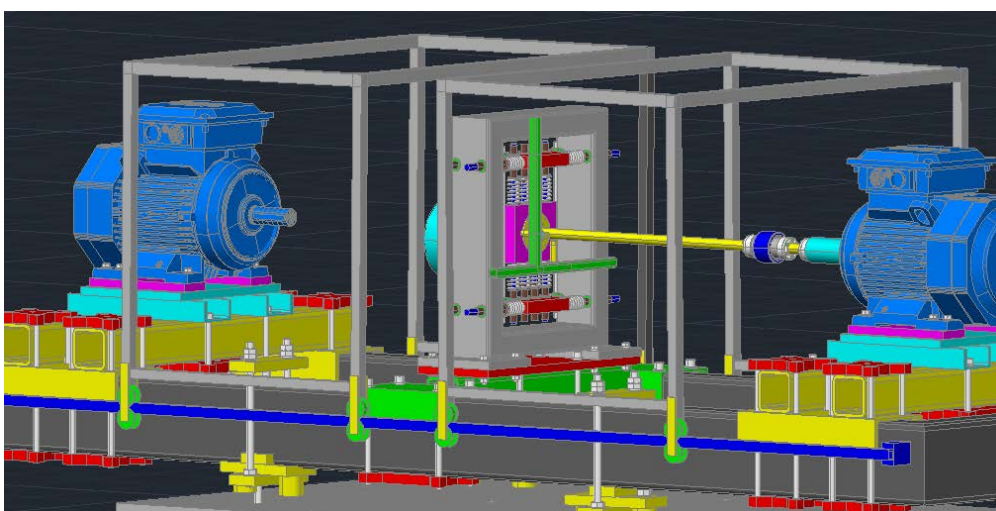

Figure 50: Safety frame virtual design

9 Accelerometer Measurements

Using the VI developed, discussed in a previous chapter, it was possible to extract the raw data that the sensors were recording from the responses of the test rig. As an initial test assessment into the acquisition sampling rate (Hz) was made, to determine what would deliver the best data representation. The results from this experiment are shown in Figure 51 and Figure 52.
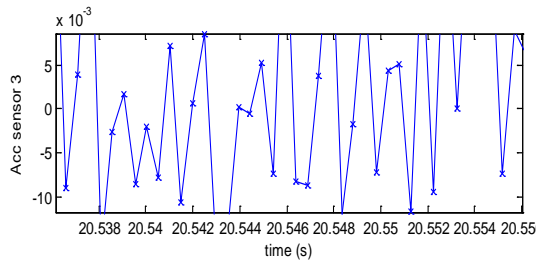
Figure 51: 2k sampling rate
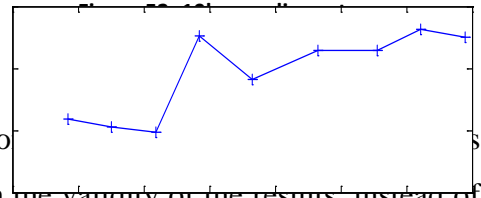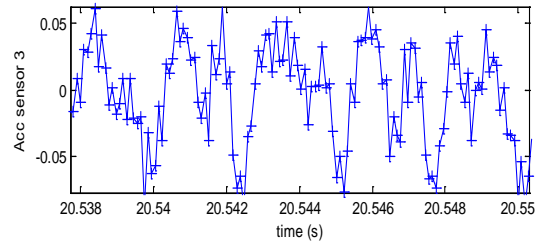
In Figure 51 and Figure 52 an increase in acquisition ... alteration generates a significant improvement in the validity of the results; instead of the signal appearing random; a periodic wave form can be identified. It could be concluded that all subsequent testing would be undertaken using the 10,000 Hz rate.

Identifing an appropriate method to analyse the data obtained by the accelerometers was also important. Figure 53 and Figure 54 show the plots of the raw data as it was recorded from the sensors in both the vertical and lateral directions.
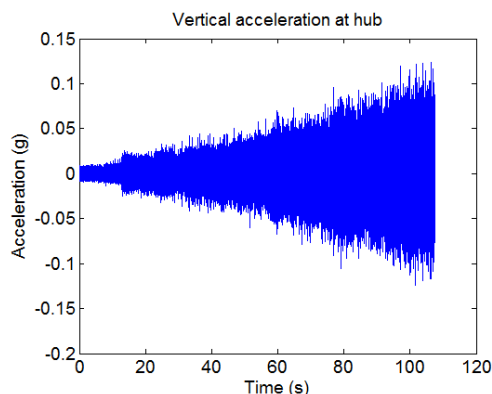
Figure 53: Obtained vertical acceleration data
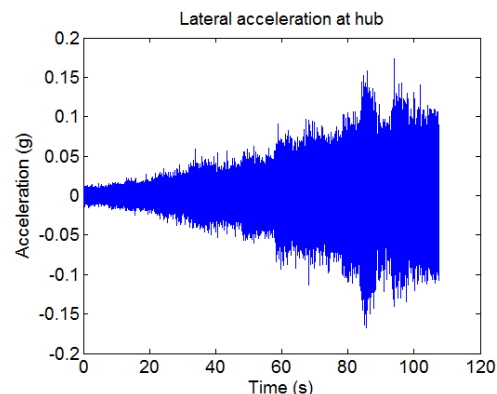
Figure 54: Obtained lateral acceleration data

The very first analysis method calculated, the Root Mean Square (RMS), is a statistical measure into the magnitude of a varying quantity. The problem with this approach was that the readings were becoming heavily distorted by the noise level on

the system, higher orders of vibrations from the motor were exciting the eigenmodes at higher frequencies. This should have been visible in the RMS results however the general noise was "blurring" the response.

As a secondary analysis method the Frequency Response Function (FRF) was taken, the results are shown in both the vertical (Figure 55) and the lateral (Figure 56) directions. This is the response of the system for a specific frequency and is a type of transfer function, i.e. input to output relation as a function of excitation frequency. The specific frequency corresponded to the motor input frequency. Eigenmodes, i.e. resonances, are particularly sensitive, and are seen as spikes or mountains in the FRF. Excitation at such frequency is expected to give large vibrations (steel frame = low damping), which can affect the sensors or the whole system, if there is little noise in the signal, and there is a pronounced eigenmode. The problem is likely that the excitation is not just a single frequency. It probably contains many different frequencies, and the sensors pick up different kinds of noise. An alternative to the stepped function input that acts as a frequency sweep is to have a wide-spectrum excitation, also known as a "knock test", this will be discussed in a later chapter.
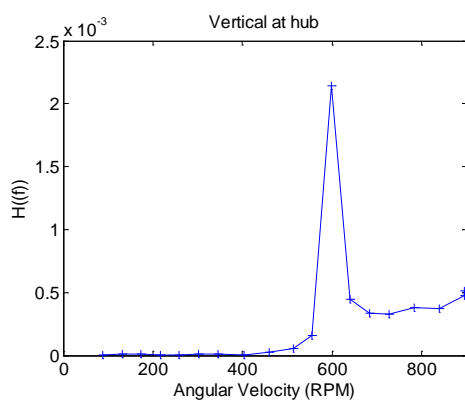
Figure 55: Processed vertical acceleration data
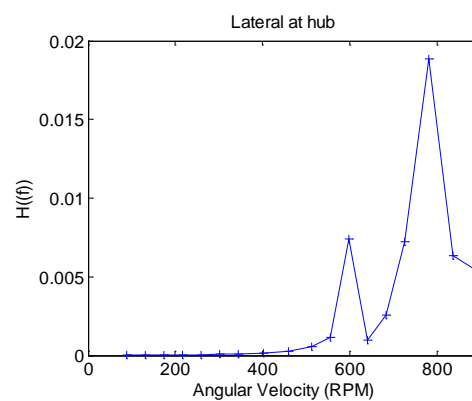
Figure 56: Processed lateral acceleration data

9.1 Accelerometer Robustness Tests

Before full operational testing was carried out it was important to consider the accelerometers abilities and performance capabilities. It was important to assess the performance of the accelerometers under varying operational scenarios, including relocations and disturbances. It was from this that a series of sensor robustness checks were undertaken. A stepped function, shown in Figure 57, was delivered to the test rig

as the operational scenario using a predefined VI developed in Labview and all analysis was then conducted using Matlab.
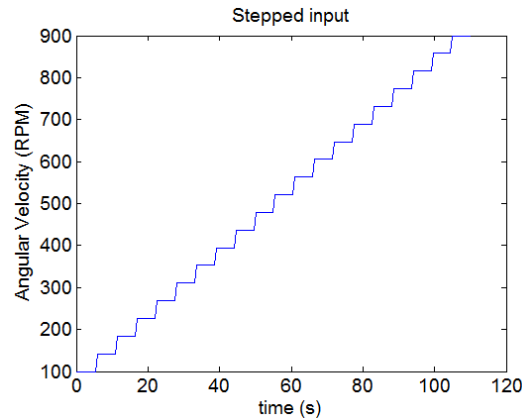
Figure 57: Motor input - stepped function

A preliminary set of tests were conducted that sought to identify the robustness of the accelerometers. An input of a twenty stepped function from 100rpm to 900rpm was inputted to the system and varying disturbances were made on the accelerometers. The first set of results indicated as '*Orig data*' in Figure 58 and Figure 59 below acted as a base set of values for the next tests. The second test that was undertaken aimed to identify the implication of a disturbance to the sensors. All sensors were lifted and repositioned in the same locations as they were for the first test. The recorded data is plotted as '*Replace*' in Figure 58 and Figure 59. The third test that was carried out aimed to identify whether there was any noticeable difference in the recording capabilities between the high sensitivity (500mV/g) and low sensitivity (100mV/g) sensors. All three tests had data recorded in the lateral and vertical direction and the recording sensors where positioned on the top and side of the bearing hub.
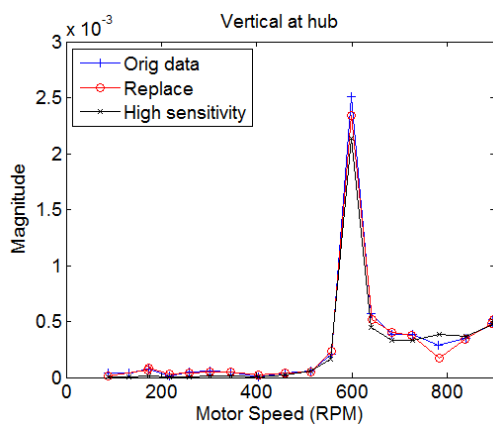
Figure 58: Vertical accelerometer robustness response
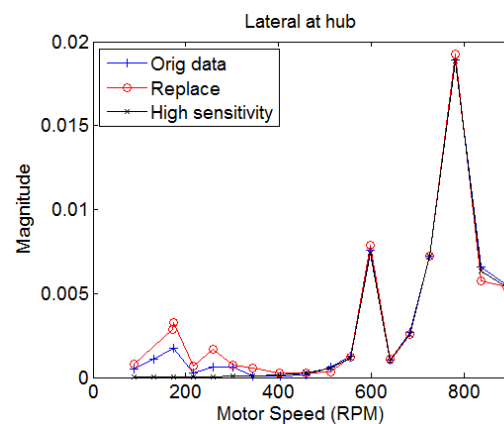
Figure 59: Lateral accelerometer robustness response

From Figure 58 and Figure 59, a close correlation is identifiable from the data recorded over the series of preliminary tests show. There are small deviations in the lower rpm values on the lateral recording however the two focal points at 600rpm and 780 rpm are consistent. The preliminary test allows the conclusion to be made that the accelerometers are recording very similar data as one another and that a full disturbance (such as removal and replacement) had very little alterations to the recording effectiveness.

9.2   Accelerometer Response for Varying Motor Speed

The next set of tests undertaken aimed to investigate the data comparison between accelerometers when they were positioned around the test rig. These tests were conducted using the pair of high sensitivity sensors, one in the vertical direction and the other in the lateral direction.

The prediction made for this experiment was that the vibrations recorded would decrease as the distance from the bearing hub was increased. The reason for this expectation stemmed from the idea that the shaft is contacting the bearing hub first, so all vibrations originate from there. Another assumption drawn is that objects shake more the further away from their point of fixation, particularly if they are light, which the test rig is.

The first data recorded had the sensors positioned on the vertical and horizontal bracket arms of the test rig. These were then repositioned the sensors on the top and side of the bearing hub, before moving them onto the test frame and finally onto the table. The data obtained is graphically represented in Figure 60 and Figure 61.
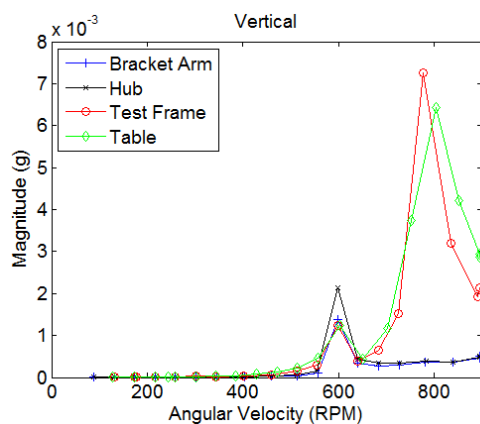
Figure 60: Vertical accelerometer location response   Figure 61: Lateral accelerometer location response
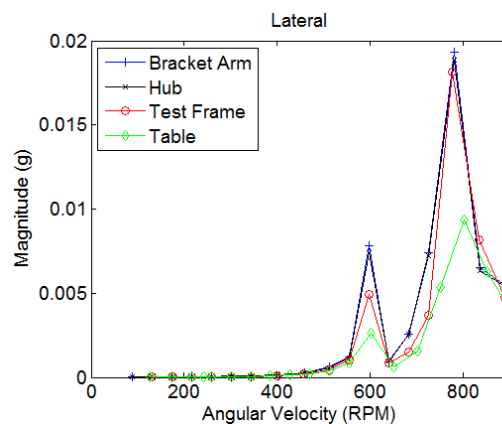
By analysing the results of the lateral direction data first, it can be identified that the hypothesis made was accurate. Higher accelerations are visible on the bracket arm and the smallest accelerations were recorded on the table. Controversially the data measured in the vertical direction, only matches the hypothesis made up to 600rpm. Beyond this value it is clearly identifiable that a reverse in the predictions made occurs with the highest accelerations being found at the test frame and table with very small recorded values being obtained on the bracket arm and the bearing hub.

An explanation for these results could be drawn from the excitation force that is being applied to the system. In the vertical direction a presumption can be made that the excitation force is no longer from the shaft and is in fact from the motor itself. This is located on top of the test frame which is then connected to the table before its connection to the bearing hub. This first connection to the table could be acting as a nodal point creating the next highest recorded amplitudes on the table, after the vibrations have transferred through the system to the bracket arm and bearing hub they have reduced significantly in amplitude.

It can be concluded from the tests, that the sensors all perform to a similar performance level despite the clear differences in sensitivity ratings. It can also be suggested that the location choices of these sensors with respect to their sensitivity levels can be ignored. Consideration however, must be given to the data recorded in the vertical direction in future tests.

10 Knock Tests

In order to investigate the eigenmodes of the system, two separate test types were undertaken, the stepped accelerometer tests that were discussed previously as well as knock tests. These tests were conducted to build the force response function of the system in a variety of areas. The stepped tests were designed to capture the connections to the motor, for example the shafts, motor mount and bearing hub structure, compared with the knock tests that were designed to analyse the frame structure itself.

A better knowledge into the systems structure needed to be developed. In order to achieve an understanding into how the system operated under varying cyclical loading tests a series of knock tests were undertaken to analyse the systems eigen frequencies. Any eigen frequencies that are contained within the structure and are excited by system in balances have the potential to cause measurement problems through the amplification of the frequencies recorded.

Using the block diagram shown in Figure 62, the capture of the frequency spectrum created from the knock test was possible. The DAQ assistant was connected to the physical channel containing the accelerometer, this was connected to a "trigger and gate" module. This module uses a trigger to extract a signal segment. This segment was predefined using a series of input controls including start level, hysteresis and stop level. For this series of tests, a start level of 5 was used, which indicated the amplitude level that the signal had to pass before the trigger was initiated. As a preliminary read out, the module recorded the previous 10 samples before the trigger opened, this was used as a visual validation that initiation had occurred at the correct time. A hysteresis level specified the level above or below the start value that needed to be obtained to initiate the trigger; this was set to 0 as the start level of 5 was sufficient. The closing of the gate was set using the sample number required of 1000.

After the Trigger and Gate module, the FFT unit was explored. The "Fast Fourier Transform" unit computed the FFT spectrum of the signal and returned the results as magnitude and frequency. This was incorporated as a means of identifying the eigen frequencies within the system.
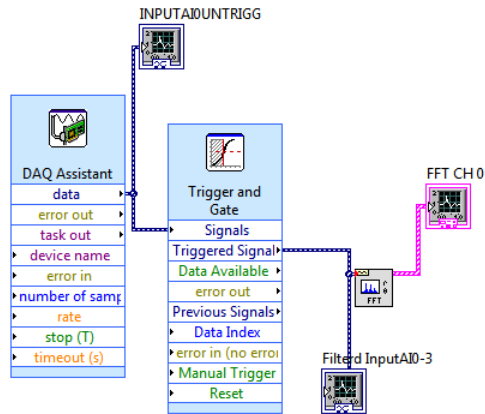
Figure 62: Knock test Labview VI

Several tests were undertaken around the system, however for ease of data collection, a discussion of the results obtained by three of these tests will now be made.

The initial test aimed to assess the eigen frequencies within the test frame. This was an important test to analyse whether vertical bending would have an influence on the results obtained from the operational system. An accelerometer was positioned behind the HSS motor the rig was then contacted behind the disconnected motor allowing for a full test frame analysis. The results from this experiment are shown in Figure 63.
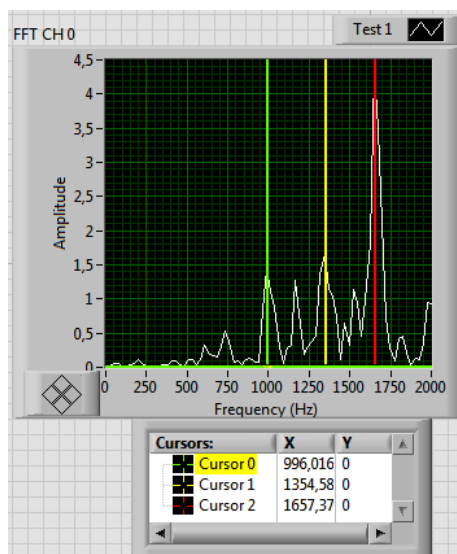
Figure 63: Knock test 1

The action of the motor engaging will deliver a range of frequencies into the system from 0Hz to 50Hz. It is identifiable from the Figure 63 that there is no notable eigenmodes recorded at these frequency levels and therefore no concern about the system being excited by the bending of the frame.

The second test undertaken was an analysis into the eigen frequencies contained within the bearing hub and their effect on future acceleration tests on the bracket arm.

Figure 64: Knock test 2 location
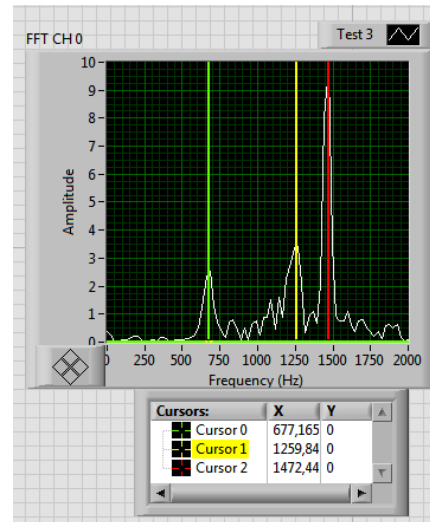
Figure 65: Knock test 2 results

Similar conclusions can be drawn to the first test carried out, in that the eigen frequencies obtained are far higher than the motor delivery frequencies.

The third and final test carried out followed a similar strategy to the second test. Understanding needed to be made into the eigen frequencies contained within the bearing hub in order to identify their effects on acceleration recordings made on the vertical bracket arm. Figure 66 is a photograph identifying the positioning and the point where impact was made; a yellow ring highlights the accelerometer location. The graphical results obtained are shown in Figure 67.
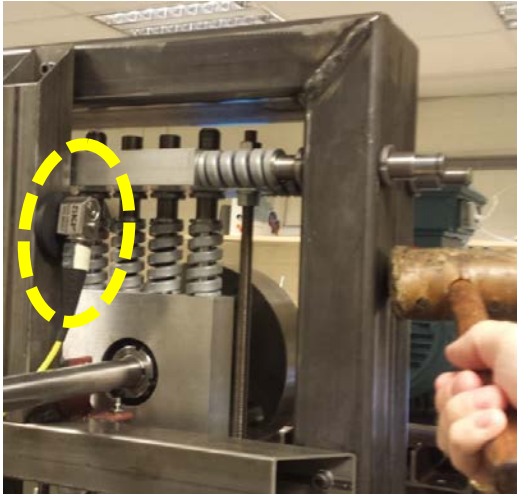
Figure 66: Knock test 3 location
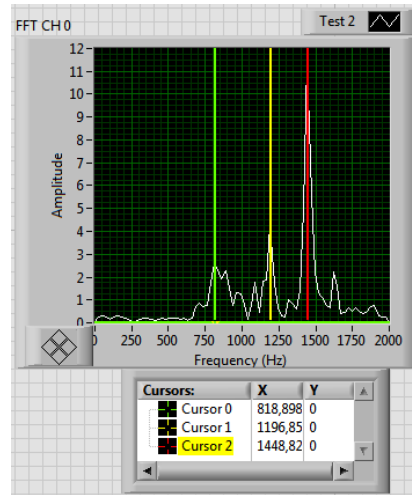
Figure 67: Knock test 3 results

Having eigen frequencies that exceeded the motor output level meant that there was no excitation occurring. The values obtained relate very closely to the second test conducted on the horizontal bracket arm. Under a "perfect" sinusoidal motor, one main eigenmode should be notable, it is however important to identify that the motor will exhibit certain overtones that can be integer multiples of the excitation. These corresponding to motor speed, creating these higher order frequencies required to excite the frame eigenmodes >750 Hz.

As a conclusion to the results obtained and all the other tests carried out, it can be said that the frame is stiff enough so that it is free from low frequency eigenmodes, therefore no impact will be made on the experimental results obtained.

11 Displacement Probe Analysis

The results from the previous tests involving the accelerometer responses and knock tests were a way of ensuring that the displacement sensors would give reasonable results with little influence from other factors. The data obtained from the displacement probes would be used in the evaluation of the computational model so the analysis of the displacement probes formed another key evaluation area. The preliminary tests were developed in order to enhance the understanding of what was actually happening at the displacement sensors.

These series of tests were designed to analyse the effectiveness of the voltage displacement probes. With the results obtained, analysis could then be made into the contribution of noise of the system under various operational scenarios.

After the results of the vertical probe test, discussed in a previous chapter, were analysed, it could be concluded that an alteration in the voltage reading of 1V corresponded to a displacement of 0.361mm for the shaft. The first test undertaken was a static shaft test, with the aim of highlighting what voltage alterations could be associated with system noise. Noise on a static shaft system would still correspond to displacement values being obtained.

The first test scenario ran for 20 seconds and the displacement probes recorded all the data relating to a static shaft. The results are shown in Figure 68.
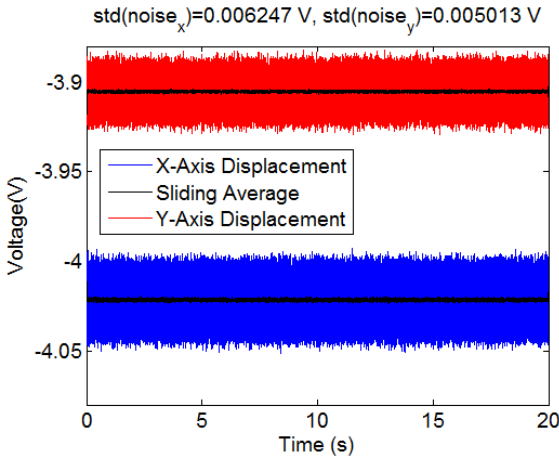

Figure 68: Static shaft test results

When analysing this data in Matlab, a command was used that plotted the sliding average. This method took a sliding average for the data points and could be used as a technique of

removing the noise from the system. An appropriate value for this plot was to use an N-Slide value of between 25 and 50. It was deduced from other assessments that a value <25 then noise still dominated the signal response and a value >75 lost the signal detailing. A value of 50 was used in all subsequent analysis so that each data point in the displacement data was replaced by the mean of the 50 preceding recorded points and 50 subsequent points. This value of 50 corresponds to 0.005 seconds which relates to the sampling rate of 10,000 per second (10k). If the value of sampling rate is altered then the value of n-slide will also need to be altered, for example a 1k sample rate would require the n-slide value to be changed to 5.

I also calculated the standard deviation, which is the spread from the sliding average values for a series of data, the smaller the value the greater the central tendency meaning that the data is concentrated around mean, the higher the value the greater spread of data. The results from this static test show a small value indicating that the data is concentrated around the mean. The response from the graphical data presented in Figure 69 is that noise on the system accounts for roughly 40 mV alterations (standard deviation = 6 mV) in the X-axis displacement probe and around 30mV (standard deviation = 5 mV) in the Y-axis displacement probe. It is expected that the "visual noise" level and the standard deviation values should be proportional.

A second test was developed as an identifier to see if very slow rotation on the shaft would have an effect on the noise experienced on the system. The shaft was hand rotated three times over a period of 25 seconds and the data recorded. Matlab analysis generated the graphical data shown in Figure 69.
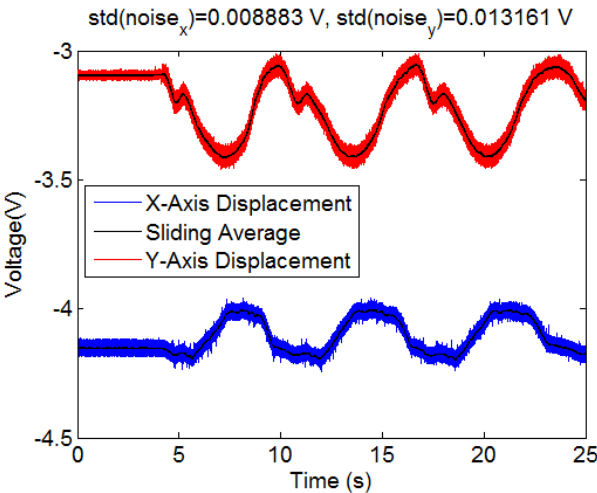

Figure 69: Shaft hand rotation results

The graphical data shown in Figure 69 identifies that the voltage alterations appear similar in magnitude to the static shaft test performed previously. Noise represented alterations of

around 50mV in the X-axis (standard deviation = 8.8 mV) and 35mV in the Y-axis (standard deviation = 13.1 mV). The standard deviation results were not as expected and did not agree with the predictions that were made about the proportionality increase from the previous experiment.

The series of further test were undertaken with the priority to identify how much noise was accountable by a motor that had brakes engaged. A motor that had the brakes applied gave the same response scenario as a static shaft but with the addition of noise interference from the motors electrical cabling. The results obtained indicated a significantly larger noise level on the system with the motor incorporated into the system. Observing displacement voltage readings of around 150mV in both axial directions identifies that an approximate addition of 100mV of noise has been added into the system by the introduction of a braking motor.

The final noise analysis test acted as a combination test where the shaft was being slowly driven by the motor. This incorporated aspects of the still shaft, braking and rotation into one experiment. The Labview VI controlled the motor to spin at one revolution per fifteen seconds, while the data was being acquired. In this instance an addition of approximately 150mV has been added into the system on top of the static motor noise by having the inclusion of shaft rotation.

The outcome of these experiments is that the factoring of noise into the results must be actively considered within the data analysis phase.

12 Shaft Tests

After the completion and analysis of the static tests, it was time to test the rig under an eccentric load conditions. The eccentric (E) load conditions were developed in parallel to the computer model development, allowing for both the model and reality to be compared together.

The initial test consisted of two inputs to the system, a stepped function and a ramped function. Both tests together would cover a wide range of operation scenarios that could be present on an operational wind turbine out in the field. These inputs are graphically displayed in Figure 70 and Figure 71 below.
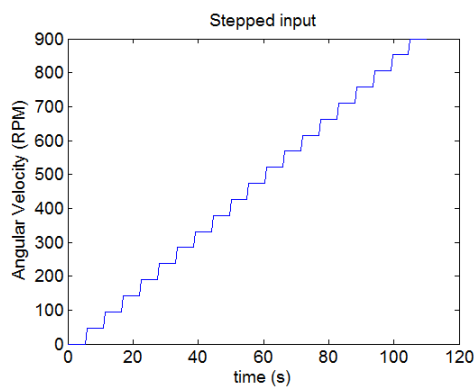
Figure 70: Stepped motor input
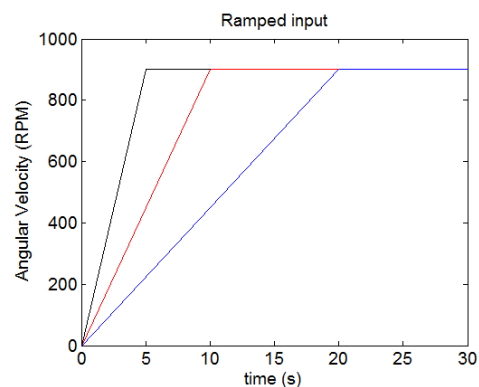
Figure 71: Ramped motor input

The stepped function was created with a stepping time of 5 seconds creating a total run time of 110 seconds. The ramps were predetermined to allow a range of gradients to be achieved. They all ran from 0rpm to 900rpm with a transit time of 20 seconds, 10 seconds and 5 seconds respectively and a trail time of 10 seconds.

The hypothesis from this test was based on the same hypothesis used in the design of the computational model. That the system behaves with a rigid shaft and a damping spring system that operates in the bearing hub. Figure 72 gives a visual interpretation of this prediction.

Figure 72: System prediction 1 diagram

The first test was the 20 step function initially with no eccentricity (NE) followed by an eccentric (E) mass of 74.4g added to the system. The results were recorded for both the X-

Axis displacement probe as well as the Y-Axis displacement probe. For analysis purposes consider the Y-axis displacement probe shall be considered. NE is shown in Figure 73 and E in Figure 74.
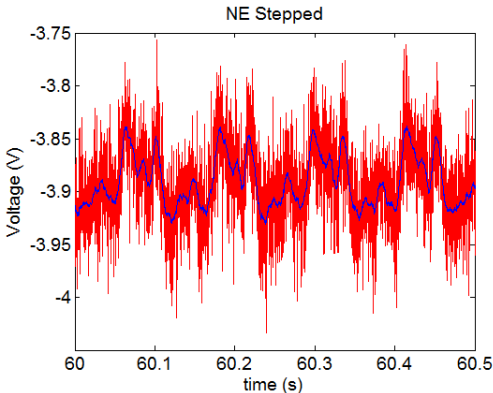
Figure 73: Vertical stepped NE response
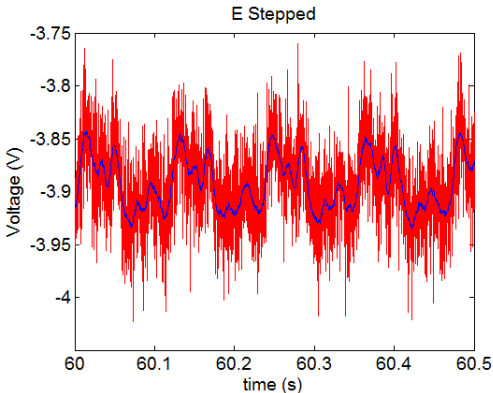
Figure 74: Vertical stepped E response

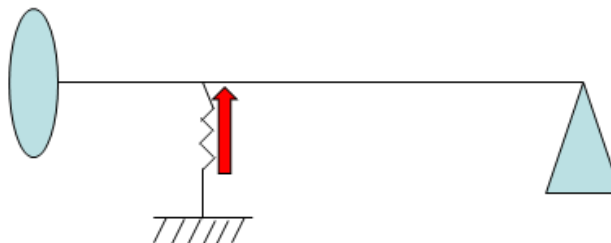Through analysis of the signal it is identifiable that the responses in the Y-Axis displacement sensor are nearly identical with and without eccentric mass. Thus suggesting that even with an eccentric mass, the system isn't creating significant displacements at the bearing house. The calculated displacement, with and without eccentric mass, equated to an alteration between the maximum and minimum values of 0.029mm.

The next test undertaken consisted of the same setup as the first test, this time the input was a ramped function. The ramped function was used for analysis purposes because it is a ramped function that is used in the computational model. Analysis was made using the 20 seconds to 900rpm ramp. The analysis between the time frame of 12.5 and 13 seconds has been selected because in the stepped test this is the point where the motor has achieved approximately 500rpm NE is shown in Figure 75 and E shown in Figure 76.
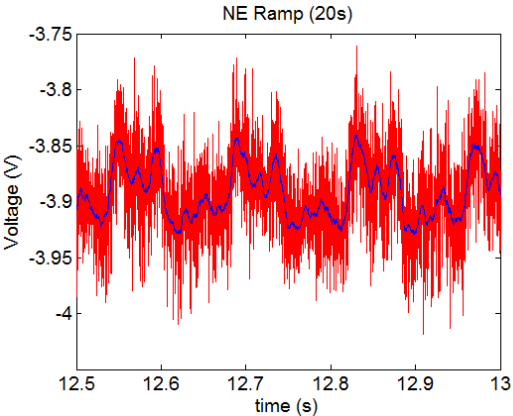

Figure 75: Vertical ramped NE response
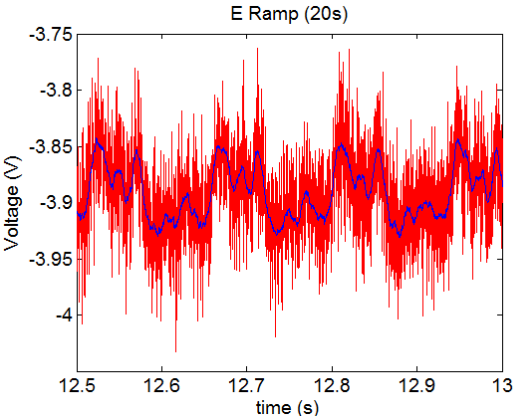
Figure 76: Vertical ramped E response

Again it is clear that similar results to the stepped assessment have been achieved with very little displacement alterations with the eccentric mass addition. This time similar displacements were recorded of 0.028mm. This could relate to the fact that the mass addition of 74 g is too insufficient to be noticeable, it was therefore concluded that heavier masses should be incorporated into future tests carried out.

The conclusion drawn, the initial prediction of a rigid shaft and spring damper system was in fact inaccurate.

12.1 Shaft end

The next test undertaken was to identify whether or not the shaft was being subject to bending after the bearing hub. To do this another displacement sensor was positioned behind the bearing house as shown in Figure 77. This time the test would be conducted under a constant frequency. It was decided that 28Hz was appropriate, equating to 560rpm. This value sat just below the critical speed of 600rpm where there was considerable visual shaking on the test rig.
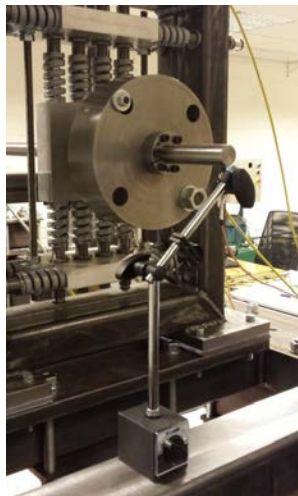
Figure 77: Shaft end displacement probe

The hypothesis for this experiment was that the system would show characteristics of bending after the bearing hub, indicating that the shaft was acting as a rigid body. Also that the damping system was rigid, forcing the shaft to deflect after the bearing hub. This is depicted in Figure 78.

Each arrow depicts the displacement sensors positioning on the test rig. The test was conducted using no eccentricity (0g), 74.4g and 353.6g in order to determine whether higher

masses would cause displacements at the bearing hub. The plotted results for varying eccentric masses are shown in Figure 79 through to Figure 81.

Figure 78: System prediction 2 diagram
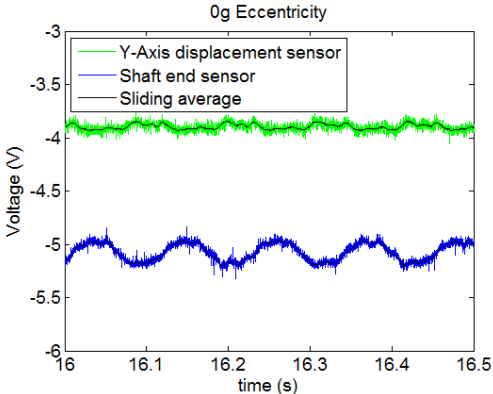
Figure 79: NE shaft response
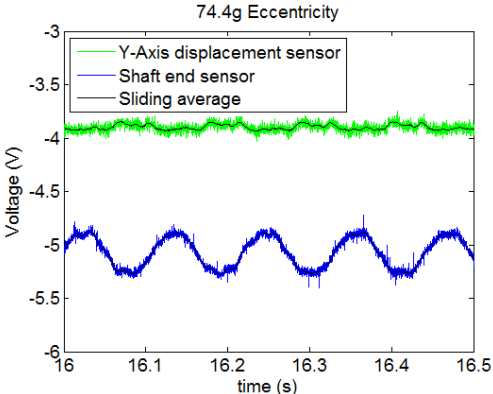
Figure 80: 74.4g shaft response
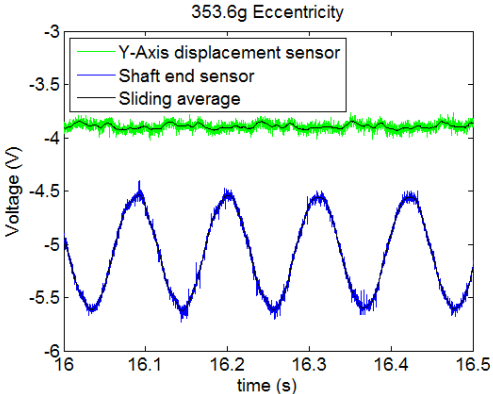
Figure 81: 353.6g shaft response

The conclusion that can be made about the results shown in Figure 79 through to Figure 81 is that the shaft is showing significant signs of bending after the bearing hub. The voltage alteration of 1.1V shown between 0g and 353.6g equates to a displacement of 0.397mm which is a significant alteration when compared with the voltage change at the vertical (y axis) displacement probe which showed virtually no alteration in the voltage change at all.

12.2 Mid shaft

After the previous test, there was now concern about the shaft pre-bearing hub (between coupling and bearing house). The third and final system test that was carried out aimed to identify if the shaft was bending before the bearing hub, over the length of shaft connecting the motor with the coupling and onto the bearing hub.

To do this another displacement sensor as then positioned the middle of the test shaft (near to coupling), this is shown in Figure 82.
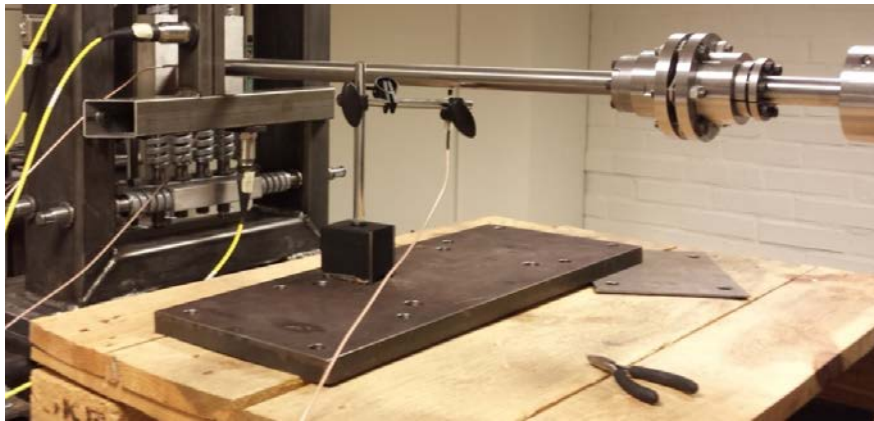
Figure 82: Mid shaft displacement probe

For this test an input frequency of 27 Hz was used equating to 540 rpm. This value was selected because now there was a new critical speed of 560 rpm. The probable cause for the alteration from previous test was due to the structural change required to conduct this test.

The hypothesis for this experiment was that the system would show characteristics of bending after and before the bearing hub. During the transition through the bearing hub it is predicted that the shaft will remain rigid so small displacements will occur. This will verify that the damping system is rigid which is forcing the shaft to deflect before and after the bearing hub. This prediction is depicted in Figure 83 where the arrows indicate where the additional sensor was positioned. The same tests that were previously carried out were undertaken again and the results with varying eccentric masses are shown in Figure 84 through to Figure 86.
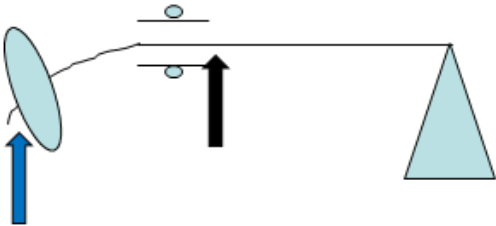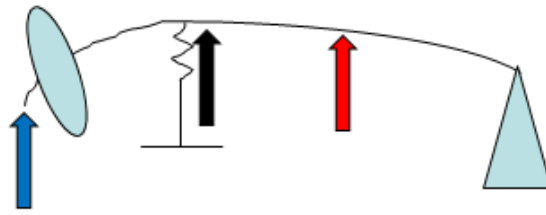
**Figure 83: System prediction 3 diagram**
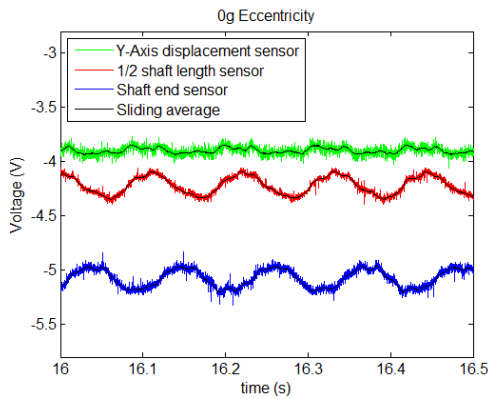
Figure 84:NE shaft response
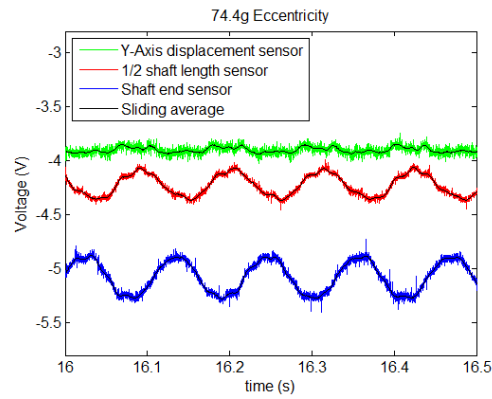
Figure 85: 74.4g shaft response
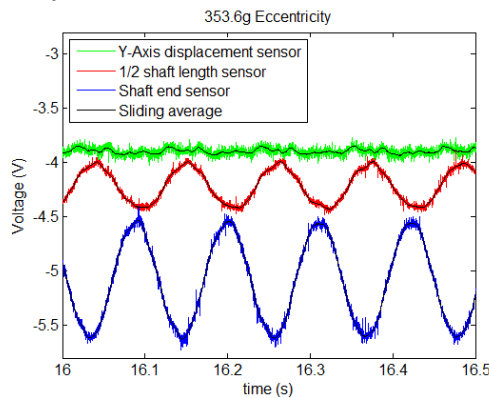
Figure 86: 353.6g shaft response

Many conclusions can be drawn from the results shown in Figure 84 through to Figure 86. The first is that as the eccentric mass value is increased, it is possible to see a greater deflection created in the shaft after the bearing hub. The difference between the 0g and 353.6g experiments, show a displacement increase of 0.314mm at the end of the shaft.

Contrary to this, the sensor that was positioned half way along the shaft sees very little alteration in its displacement characteristics, with a displacement increase of 0.063mm between 0g and 353.6g. Identifying that even with no eccentricity (0g), a displacement is visible, led to the suggestion that the shaft may in fact be permanently bent. This directed the following test to be conducted into the symmetry of the shaft.

12.3 Shaft Symmetry Test

After the conclusions that were drawn from the previous set of tests it was important to now identify why it was that in the previous tests a non-eccentric test yielded results that indicated a 'half shaft length' displacement of 0.063mm.

In order to assess the symmetry of the shaft an Ironside mechanical gauge was used that was capable of measuring displacements up to 0.01mm [19]. This mechanical gauge was positioned at points along the shaft, the shaft was slowly rotated and the point corresponding to the highest displacement change was noted. The mechanical gauge was then moved 10cm along the shaft and the test was repeated. The prediction for this test related to the results of the previous eccentric test, in order to identify the shaft bend the dots should be in a straight line along the shaft length with varying degrees of magnitude. If the shaft was "ideal", and the only bend was caused by the weight of the disc then no maximum deflection would be detected. Figure 87 the mechanical gauge used and Figure 88 shows the result values obtained.

Figure 87: Ironside mechanical gauge
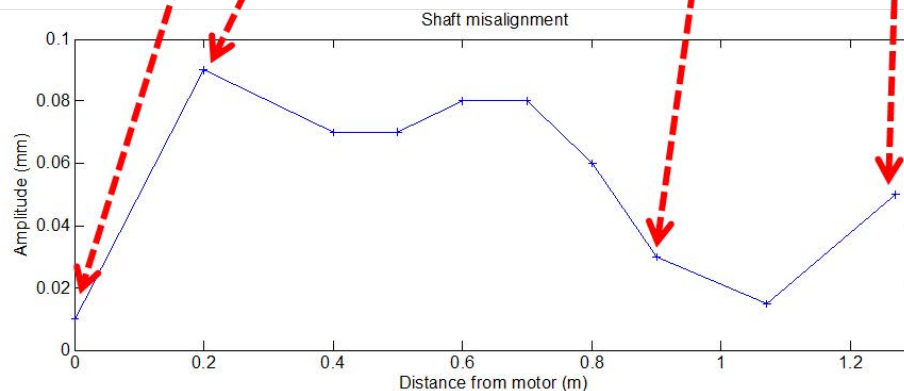
Figure 88: Shaft misalignment results

From the results depicted in Figure 88 it is clear to see that the shaft has been significantly bent before bearing hub. A bend is identifiable post bearing hub with a deflection magnitude of 0.05mm present. One problem with this testing method is that each recorded point is being measured with relation to the centreline of that object. If it is in fact the centrelines that are not aligned then this test will give very inaccurate data. As a future test consideration, these displacements should be recorded with relation to each individual component. Alterations to the test rig could then be made to reduce this level of centreline misalignment.

The next test carried out aimed to asses at what rotational positioning these maximum displacement readings had taken place. A clock face was attached to the motor face plate and a corresponding angular value was recorded from the vertical position for each of the data points on the shaft. The results of this test have been plotted in Figure 89.
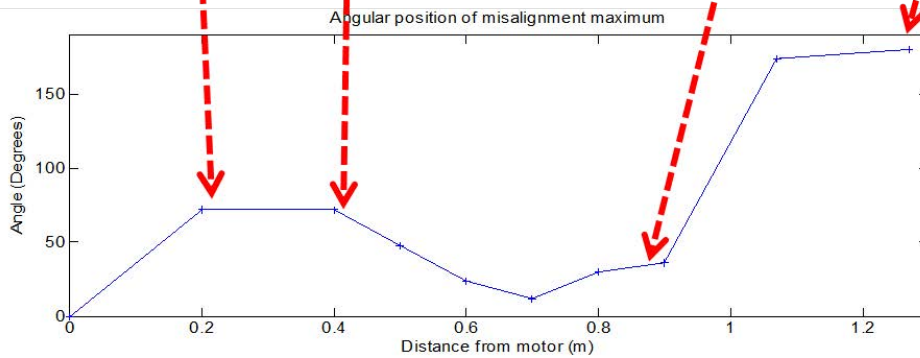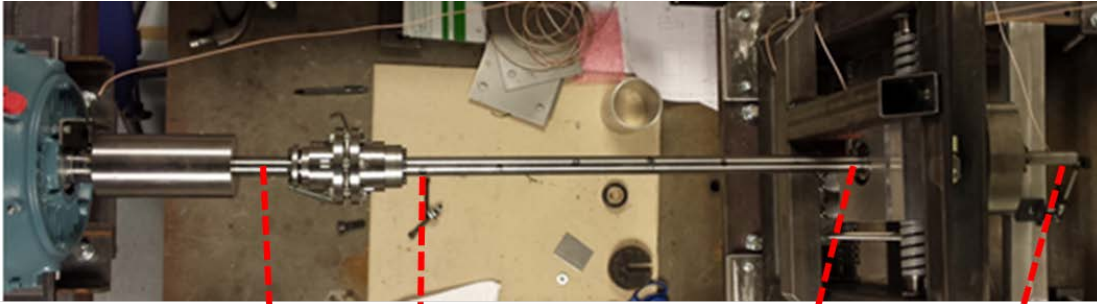
Figure 89: Angular maximum position response

Figure 89 highlights a considerable twist on the system. From the main shaft start to finish there is a recorded angular alteration of 180 degrees between these two maximum displacement points. The cause for such a twist is unknown, however proposals, that this occurred during the production process, have been suggested. Future analysis should be made into this anomaly to identify the cause.

13 Conclusion

The initial design and fabrication of this test rig was conducted by another student and the design team at Chalmers, further progression from this basic setup was required in order to enhance the operational capabilities of the test rig.

This development began with the priority of identifying the key areas for improvement. Initiating with the development route strategy, this assisted in the projects progression, following with the hardware and software development.

Further structural enhancements were required for the test rig, with designs for sensor positioning allowing for this. An in-depth understanding and knowledge of the sensors calibration and capabilities has since been developed, with an indication for their usable parameters being available for all future test rig operators and researchers.

A range of probes have since been connected onto the test rig and data acquisition routes have been developed and incorporated into the overall system. Analysis into the test frame responses under varying operational scenarios has been undertaken with a view to identifying vibrational causes of misalignment.

A full shaft investigation helped to identify key induced misalignment areas of the system that will be used in the future work of the mathematical model development.

The project, following the guidelines of the master's programme, can be considered to be multidisciplinary in its orientation. It is important to identify that a considerable level of electrical understanding was required for the project. Expressed in the form of hardware testing, knowledge of oscilloscope operations, voltage dividers and motorised machinery. Heavy project direction was emphasised as being mechanically related, with engineering topics such as system dynamics, statics and condition monitoring were all utilised in the development of this test rig.

A series of engineering software packages have also been integrated into this project. Mathematical calculations were undertaken in both Matlab® and Excel®, 2D and 3D models were constructed in AutoCad®, data acquisition took place using National Instruments Labview® and the SKF @ptitude Observer®. All these packages will continue to be used in the development of this test rig, with the incorporation of other software such as ADAMS® for the mathematical model development.

This report, Chalmers, Applied Mechanics, Master's Thesis 2014:36, will serve to educate future test rig operators, users and other readers on the appropriate methods for data acquisition from this test rig and other drive train systems. Aspects will prove insightful for research conducted in the energy and design industries as well as in academia.

Professionalism was maintained throughout the course of this project. Seminars were scheduled once a week for 90 minutes to discuss the projects development, direction and key target areas. A series of meetings and discussions were also held with the industrial partners of this project to identify the scope and requirements. A proficient manner was also taken to address paper work and document unity. All parties associated with the projects progression and development were given access to the Dropbox® file sharing service where all relevant documents, designs, order sheets and conformity papers were uploaded, this helped to integrate everyone with the projects progression.

It can be considered that the initial objective set out at the project initiation has been achieved. It is however important that the overall project progression is maintained in keeping with the overall deadline plan. Consideration therefore has to be given to the future requirements.

15 Future Outlook

After undertaking the development of the test rig to its current stage it is important to consider the future developments that can be undertaken.

Beginning with the completion of the safety casing frame, it is important that this is completed before the WindCon system is installed during the training package that will be delivered by SKF. It is imperative that safety in maintained during this training because there are many hazards present with the laboratory.

The next level of progression should be directed to completing the installation of the second analysis path, the SKF route. Beginning with the installation of the IMxP-multi-log system and incorporating the signal dividers to keep the NI system operational, simultaneously with the SKF system. This future enhancement should be closely combined with the development of software sets, Labview and @ptitude Observer.

The next development is the progression of the test rig into its second setup phase, it is this setup that will act as a model for the direct drive wind turbine. At this stage, analysis can take part on a number of dynamical aspects, including shaft torque, bending moments and the effects of angular misalignment.

Progressing further on from this could be the development and analysis of setup three. At this stage is where all of the finite analysis can be made which is directly comparable to a full scale wind turbine. By incorporating a modular and interchangeable gearing system, analysis could be made into the effects and efficiencies of power transmission using parallel spool gears or a planetary gear set. Coupling with the effects of misalignment on the system and a very in-depth analysis can be made.

As another future consideration, studies could be taken into the effects of the interaction of mechanical components (coupling, shaft, etc.) and electrical components (motor, etc.) within the system. Particular attention could be made into the effects of stray currents passing through the bearing housing and the effects this has on the performance of the rotational capabilities of the system.

As a final reflection, the results obtained from this report and all future analysis can be used as a prediction into the impact of full scale wind turbine operations. Pairing this towards the CMS currently in operation, to develop further improvements and enhancements.
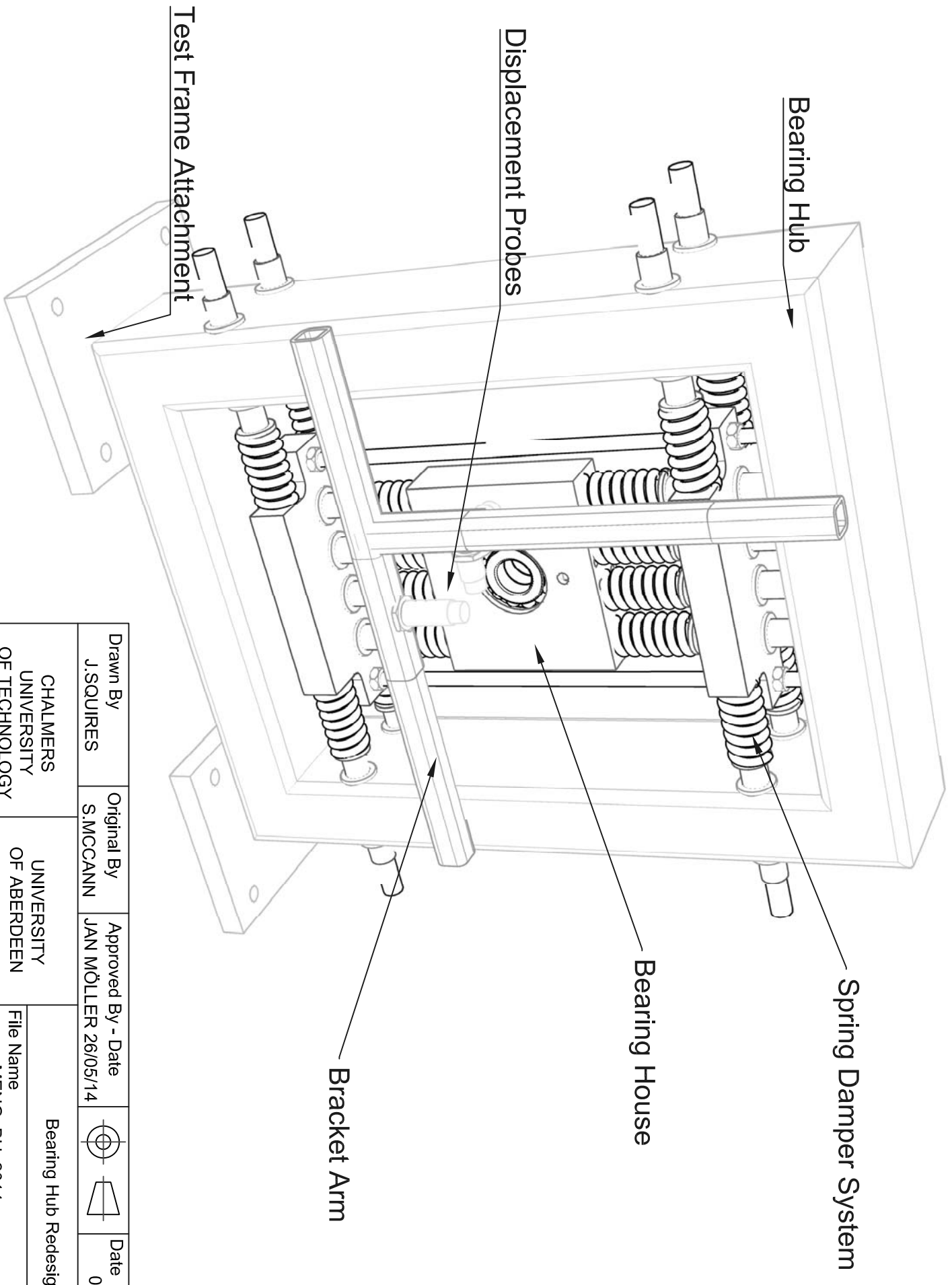
References

[1]   ABB ACS355 drives *User's manual*, 2012 49-310 pp. Catalog

[2]   Report: Pineda, I., Azau, S., Moccia, J. and Wilkes, J. Wind in Power - 2013 European Statistics. 2014, 12 pp.

[3]   Commission, E. Renewable Energy: Progressing towards the 2020 target. 2011. Catalog

[4]   BBC (2014), 'Massive offshore wind farm in Outer Moray Firth approved', <http://www.bbc.com/news/uk-scotland-highlands-islands-26645997>, accessed 20/03/2014.

[5]   ABB Low voltage *Process performance motors according to EU MEPS*, 2013 27 pp. Catalog

[6]   ABB ABB F-series fieldbus adapter modules. *ACS355, ACS850, ACQ810, ACSM1 and ACS880*, 2013. Catalog

[7]   ABB *ABB Drives Pulse Encoder Interface Module MTAC-01*. 2006, ABB Oy: Helsinki. Pamphlet

[8]   SKF SKF Multilog On-line System IMx-P *Condition Monitoring Center* 2013. Catalog

[9]   SA, V.-M. CMSS 65/CMSS 665 Series 2010. Catalog

[10]   Inc., S.U. SKF Vibration Sensors 2013 19, 104, 129 pp. Catalog

[11]   Instruments, N. (2014), 'Installing and Configuring NI CompactDAQ Chassis', <http://www.ni.com/gettingstarted/setuphardware/dataacquisition/compactdaq.htm#NI >, accessed 15/03/2014.

[12]   Instruments, N. (2014), 'NI CompactDAQ', <http://www.ni.com/data-acquisition/compactdaq/>, accessed 02/06/14.

[13]   SKF @ptitude Observer User manual. 2012 16-139 pp. Catalog

[14]   Instruments, N. (2014), 'LabVIEW System Design Software', <http://www.ni.com/labview/>, accessed 25/02/14.

[15]   MathWorks (2014), <http://www.mathworks.com/>, accessed 03/05/14.

[16]   Microsoft (2014), 'Server and Cloud Platform - SQL Server', <http://www.microsoft.com/en-us/server-cloud/products/sql-server>, accessed 02/04/14.

[17]   Solutions, R. [RE]built wind turbine - BONUS 600kW. 2012 6-10 pp. Catalog

[18]   Linde, L. HEAVY DUTY 800 SERIES - ENCODER MODELS. Catalog

[19]   Mikrometer (2014), 'Mikrometer.se katalogen', <http://www.mikrometer.se/>, accessed 10/06/14.

[20]   National Renewal Energy Laboratory (2014), <www.NREL.gov>, accessed 29/02/14.

[21]   U.S Department of Energy, <www.energy.gov>, accessed 05/03/14

[22]   National Wind Technology Centre, <http://www.nrel.gov/wind/nwtc.html>, accessed 02/03/14

[23]   European WInd Energy Associations, <www.ewea.org>, accessed 13/03/14

Table of Appendices

Number	Description	File Name
1	Bearing Hub Model	MENG_BH_2014
2	Test Setup 1	MENG_TR_2014
3	Matlab Code	plotDataTest2

Test Frame Attachment

Displacement Probes

Bearing Hub

Bracket Arm

Bearing House

Spring Damper System

Drawn By J.SQUIRES	Original By S.MCCANN	Approved By - Date JAN MÖLLER 26/05/14	Date 03/04/14
CHALMERS UNIVERSITY OF TECHNOLOGY	UNIVERSITY OF ABERDEEN	File Name MENG_BH_2014	

Bearing Hub Redesign

Revision
1

Coupling

Table

Rolling Mounts

Eccentric Mass

Motor Mount

Test Frame

ABB Motor

Safety Frame

Drawn By J.SQUIRES	Original By S.MCCANN	Approved By - Date JAN MÖLLER 26/05/14	File Name MENG_TR_2014	
CHALMERS UNIVERSITY OF TECHNOLOGY	UNIVERSITY OF ABERDEEN	⊕ ⌓	Test Rig Redesign	Date 03/04/14
				Revision 1

```matlab
clear
close all
clc
fclose('all');

%% Read data from file.

%DataInXlsFile=true;     % set true to read from xls file
DataInXlsFile=false;    % set false to read from text (lvm) or from mat file


if DataInXlsFile

    %load AccData2
    [data,textdata] = xlsread('Data 10.xlsx');
    % Assumes 3 displacement sensors and arbritraty many accelerometers
    % each sensor has two columns, one for time and second for value

    data(:,1:2:end)=data(:,1:2:end)-min(data(1,1:2:end));
    data(:,1:2:end)=data(:,1:2:end)*3600*24;

else
    filename='test400';

    try
        load([filename '.mat']);
    catch

        fp=fopen([filename '.lvm'],'r');
        NoHeaderLines=23;
        NoColumns=14;


        for i=1:NoHeaderLines
            str=fgetl(fp);
        end

        data=nan(5000,NoColumns);

        k=0;
        str=fgetl(fp);
        while str~=-1
            k=k+1;

            str(strfind(str,','))='.';
            vals=str2num(str);
            data(k,NoColumns-length(vals)+1:end)=vals;

            if mod(k,5000)==0
                fprintf('k=%u - increasing size \n',k)
                data=[data;nan(5000,NoColumns)];
            end
            str=fgetl(fp);

            if k==150000
```

```matlab
                break
            end

            if isempty(str)
                for j=1:10
                    str=fgetl(fp);
                end
            end

        end
        data(k+1:end,:)=[];       % trimming last part

        fclose(fp);
        save([filename '.mat'],'data');
    end


end
% Call sensor 1 - 2 Bearinghub (displacement)
BearingHub=data(:,1:4);
BearingHub(isnan(BearingHub))=[];
BearingHub=reshape(BearingHub,[],4);

% Call sensor 3 KeyLock (displacement) for speed measurement
keyLock=data(:,5:6);
keyLock(isnan(keyLock))=[];
keyLock=reshape(keyLock,[],2);

% Call sensor 4 AccMeters (accelerometers)
AccMeters=data(:,7:end);



%% Find sliding average of displacement sensor and plot.

n_slide=25;
BearingHub_slide=BearingHub;
for i=1:n_slide
    BearingHub_slide(i,[2 4])=mean(BearingHub(1:i,[2 4]),1);
end
for i=n_slide+1:length(BearingHub(:,1))-n_slide
    BearingHub_slide(i,[2 4])=mean(BearingHub(i-n_slide:i+n_slide,[2 4]),1);
end
for i=length(BearingHub(:,1))-n_slide+1:length(BearingHub(:,1))
    BearingHub_slide(i,[2 4])=mean(BearingHub(i:length(BearingHub(:,1)),[2 4]),1);
end

figure
plot(BearingHub(:,1),BearingHub(:,2),'b-')
title('Disp. sensor 1')
hold on
plot(BearingHub_slide(:,1),BearingHub_slide(:,2),'r-','LineWidth',2)


figure
plot(BearingHub(:,3),BearingHub(:,4),'r-')
```

```matlab
title('Disp. sensor 2')
hold on
plot(BearingHub_slide(:,3),BearingHub_slide(:,4),'b-','LineWidth',2);
xlim([60 60.5])
%ylim([-3.8 -4.2])
ylabel('Voltage (V)')
xlabel('time (s)')
title('E Stepped')


Noise_Hub=BearingHub(:,[2 4])-BearingHub_slide(:,[2 4]);

figure            %new figure because different scale
plot(BearingHub(:,1), Noise_Hub(:,1),'b+-',BearingHub(:,3), Noise_Hub(:,2),'rx-')
legend('Disp. sensor 1', 'Disp. sensor 2')
ylabel('V')
StdStr=sprintf('std(noise_1)=%f V, std(noise_2)=%f V',std(Noise_Hub(:,1)) ,std↙
(Noise_Hub(:,2)));
title(StdStr)
disp(StdStr)

%% Determine speed if sensor 3 is at KeyLock

if true% change to true for speed measureing
figure
subplot(3,1,1)
plot(keyLock(:,1),keyLock(:,2),'ro-')
a=(min(keyLock(:,2))+max(keyLock(:,2)))/2;
inds1=find(keyLock(1:end-1,2)>a & keyLock(2:end,2)<a );
inds2=1+find(keyLock(1:end-1,2)<a & keyLock(2:end,2)>a );
if inds2(1) < inds1(1)
    inds2(1)=[];  % remove if starting on key lock
elseif inds1(end) > inds2(end)
    inds1(end)=[]; % remove if ending on key lock
end

hold on,
plot(keyLock(inds1,1),keyLock(inds1,2),'ko')
plot(keyLock(inds2,1),keyLock(inds2,2),'ko')
t_pass=(keyLock(inds1,1)+keyLock(inds2,1))/2;
subplot(3,1,2)
plot((t_pass(1:end-1)+t_pass(2:end))/2,diff(t_pass))
ylabel('T_{pass}')
xlabel('time (s)')
subplot(3,1,3)
plot((t_pass(1:end-1)+t_pass(2:end))/2,60./diff(t_pass))
ylabel('Shaft RPM')
xlabel('time (s)')
end

%% Plot and determine vibration level from accelerometers for each speed step

NoSteps=20;
t_end=AccMeters(end,1);
t_starts=t_end/NoSteps*(0:NoSteps-1)+t_end/NoSteps/3;% choose middle 1/3
```

```matlab
t_ends=t_end/NoSteps*(0:NoSteps-1)+t_end/NoSteps*2/3;% of step

freqs=zeros(NoSteps,1);
H=zeros(NoSteps,3);
H2=zeros(NoSteps,3);
for i=1:length(t_starts)
    pass_inds=find(t_pass>t_starts(i) & t_pass<t_ends(i) );
    freqs(i)=1/mean(diff(t_pass(pass_inds)));
    for j=1:size(AccMeters,2)/2
        t=AccMeters(:,2*j-1);
        step_inds=find(t>t_starts(i) & t<t_ends(i) );
        t=t(step_inds);
        u=AccMeters(step_inds,2*j);
        H(i,j)=sqrt(sum( ( (u(1:end-1)+u(2:end))/2).^2.*diff(t) ) );
        figure(50+j)
        subplot(5,ceil(NoSteps/5),i)
        L=length(step_inds);
        Fs=L/(t(end)-t(1));
        NFFT = 2^nextpow2(L);
        Y = fft(u,NFFT)/L;
        f = Fs/2*linspace(0,1,NFFT/2+1);
        plot(f,2*abs(Y(1:NFFT/2+1)))
        hold on
        harms=freqs(i):freqs(i):f(end);
        plot(harms,zeros(1,length(harms)),'rx')
        legend(sprintf('f_e=%f',freqs(i)))
        [v,kk]=min(abs(f-freqs(i)));
        plot(f,2*abs(Y(1:NFFT/2+1)))
        H2(i,j)=abs(Y(kk));
    end
end

for j=1:size(AccMeters,2)/2

    figure
    subplot(2,1,1)
    plot(AccMeters(:,2*j-1),AccMeters(:,2*j))
    ylabel(sprintf('Acc sensor %u',j))
    xlabel('time (s)')
    subplot(2,1,2)
    plot(freqs*60,H2(:,j),'+-'),xlabel('freq f (RPM)'), ylabel('H((f))')
end

%% Various plots of displacement at bearing hub

x_hub=(BearingHub(:,2)-mean(BearingHub(:,2)))*0.361188165;
y_hub=(BearingHub(:,4)-mean(BearingHub(:,4)))*0.361188165;
figure
plot(BearingHub(:,1),x_hub)
ylabel('Displacement (mm)')
xlabel('time (s)')
hold on
plot(BearingHub(:,3),y_hub,'r')
ylabel('Displacement (mm)')
xlabel('time (s)')
```

```matlab
figure
plot(BearingHub(:,1),sqrt(x_hub.^2+y_hub.^2))

figure
plot(BearingHub(:,1),(BearingHub(:,2)-mean(BearingHub(:,2)))*0.361188165)

%% Saving to mat.file for analysis

save([filename '_H2.mat'],'freqs','H','H2','x_hub','y_hub', 'BearingHub', 'AccMeters')
```